






Review

# Biomedical Applications of an Ultra-Sensitive Surface Plasmon Resonance Biosensor Based on Smart MXene Quantum Dots (SMQDs)

Seyyed Mojtaba Mousavi <sup>1</sup>, Seyyed Alireza Hashemi <sup>2</sup>, Masoomeh Yari Kalashgrani <sup>3</sup>, Vahid Rahmanian <sup>4</sup>, Ahmad Gholami <sup>3</sup>, Wei-Hung Chiang <sup>1,\*</sup> and Chin Wei Lai <sup>5,\*</sup>

<sup>1</sup> Chemical Engineering Department, National Taiwan University of Science and Technology, Taipei City 106335, Taiwan

<sup>2</sup> Nano-Materials and Polymer Nano-Composites Laboratory, School of Engineering, University of British Columbia, Kelowna, BC V1V 1V7, Canada

<sup>3</sup> The Center of Biotechnology Research, Shiraz University of Medical Science, Shiraz 71468-64685, Iran

<sup>4</sup> The Centre of Molecular and Macromolecular Studies, Polish Academy of Sciences, Sienkiewicza 112, 90-363 Lodz, Poland

<sup>5</sup> Nanotechnology & Catalysis Research Centre (NANOCAT), Level 3, Block A, Institute for Advanced Studies (IAS), Universiti Malaya (MU), Kuala Lumpur 50603, Malaysia

\* Correspondence: whchiang@mail.ntust.edu.tw (W.-H.C.); cwlai@um.edu.my (C.W.L.)

**Abstract:** In today's world, the use of biosensors occupies a special place in a variety of fields such as agriculture and industry. New biosensor technologies can identify biological compounds accurately and quickly. One of these technologies is the phenomenon of surface plasmon resonance (SPR) in the development of biosensors based on their optical properties, which allow for very sensitive and specific measurements of biomolecules without time delay. Therefore, various nanomaterials have been introduced for the development of SPR biosensors to achieve a high degree of selectivity and sensitivity. The diagnosis of deadly diseases such as cancer depends on the use of nanotechnology. Smart MXene quantum dots (SMQDs), a new class of nanomaterials that are developing at a rapid pace, are perfect for the development of SPR biosensors due to their many advantageous properties. Moreover, SMQDs are two-dimensional (2D) inorganic segments with a limited number of atomic layers that exhibit excellent properties such as high conductivity, plasmonic, and optical properties. Therefore, SMQDs, with their unique properties, are promising contenders for biomedicine, including cancer diagnosis/treatment, biological sensing/imaging, antigen detection, etc. In this review, SPR biosensors based on SMQDs applied in biomedical applications are discussed. To achieve this goal, an introduction to SPR, SPR biosensors, and SMQDs (including their structure, surface functional groups, synthesis, and properties) is given first; then, the fabrication of hybrid nanoparticles (NPs) based on SMQDs and the biomedical applications of SMQDs are discussed. In the next step, SPR biosensors based on SMQDs and advanced 2D SMQDs-based nanobiosensors as ultrasensitive detection tools are presented. This review proposes the use of SMQDs for the improvement of SPR biosensors with high selectivity and sensitivity for biomedical applications.

**Keywords:** surface plasmon resonance; biosensor; smart MXene quantum dots; biomedical



**Citation:** Mousavi, S.M.; Hashemi, S.A.; Kalashgrani, M.Y.; Rahmanian, V.; Gholami, A.; Chiang, W.-H.; Lai, C.W. Biomedical Applications of an Ultra-Sensitive Surface Plasmon Resonance Biosensor Based on Smart MXene Quantum Dots (SMQDs). *Biosensors* **2022**, *12*, 743. <https://doi.org/10.3390/bios12090743>

Received: 28 July 2022

Accepted: 7 September 2022

Published: 9 September 2022

**Publisher's Note:** MDPI stays neutral with regard to jurisdictional claims in published maps and institutional affiliations.



**Copyright:** © 2022 by the authors. Licensee MDPI, Basel, Switzerland. This article is an open access article distributed under the terms and conditions of the Creative Commons Attribution (CC BY) license (<https://creativecommons.org/licenses/by/4.0/>).

## 1. Introduction

The rapid improvement of technology, in line with the growing needs of modern societies in today's world, has paved the way for the development of the factors involved and lifestyles. Sensors are devices that help researchers in various fields such as industry, agriculture, etc. to achieve certain goals by measuring predetermined parameters. Biosensors are a special category of sensors used to study and detect chemical and biological parameters. The diagnosis of diseases, the discovery of new drugs, and the identification of contamination by biological factors such as DNA, proteins, antibodies, enzymes, and

viruses are performed by systems called biosensors. Based on their operation, these sensors are classified into mechanical, chemical, electrical, and optical groups. Apart from these, optical biosensors are divided into labeled and label-free sensors [1–3]. Optical biosensors have several advantages, including high sensitivity and insensitivity to electromagnetic interference. Optical biosensors have also covered a wide range of substrates, including SPR, localized surface plasmon resonance (LSPR), interferometers, ring amplifiers, etc. [4]. There are certain types of biosensors that use light sources and light guidance based on different methods to achieve detection and detection objectives. One of the most common types of these sensors are biosensors that use plasmonic sensing in the design of their structure and are referred to as surface plasmon resonance biosensors. SPR biosensors stimulate the phenomenon of the oscillation of electrons in the metal-dielectric junction when their rate of motion matches the rate of motion of the incident light. This category of sensors is of interest to many researchers and scientists in this field due to their small size and optimal sensitivity [5,6]. Therefore, the development of SPR biosensors can be an important area of research to find chemical and biological substances that cause diseases or have negative consequences [7–9]. One of the most important aspects in the development of SPR biosensors may be the accurate detection of ‘target molecules’ to prevent the occurrence of disease and facilitate early medical therapy. Ultimately, this will accelerate therapeutic efficacy [9–11]. To this end, high selectivity and sensitivity are the most important properties to be considered in the development of SPR biosensors. Numerous nanomaterials, including metal NP and transition metal dichalcogenide (TMD) NP, are being investigated for the development of SPR biosensors [12–15]. Although metal NPs have been more commonly used in the past [16–19], after the discovery of carbon nanomaterials, such as graphene, these nanomaterials showed a more efficient performance than current metal NPs [20–23], and their biocompatibility can render them suitable for monitoring cell-size conditions [24–26]. However, the development of new nanomaterials for SPR biosensors is possible because the demand for nanomaterials with exceptional properties and efficient performance is constantly increasing. 2D nanomaterials, such as smart MXene, are becoming increasingly popular due to their special properties, such as physical, electrical, and chemical properties [27,28]. The term ‘smart MXene’ has been used by a number of researchers for MXene-based hybrid materials, indicating their unique application-related properties. Such unique compounds make MXene a potential candidate for the fabrication of transparent conductors. MXenes offer transmittance up to 95% in the visible and UV regions with very low sheet resistance (up to 0.01 kΩ per square). Due to their excellent mechanical properties and tunable optical properties, MXenes can be used as transparent conductive electrodes for touchscreen applications, various sensors, light-emitting diodes, and flexible displays [29–31]. Among the nanomaterials for SPR biosensors, SMQDs attract much attention due to their great potential and exclusive properties in developing SPR biosensors [32–34]. SMQDs are 2D inorganic compounds composed of transition metal carbides and possess a significant atomic layer thickness. Their exceptional properties include high conductivity and plasmonic and optical qualities [35–38]. SMQDs can be used in biomedical applications due to their biocompatibility. [39–42]. This new nanomaterial is now the best option for the development of SPR biosensors in biomedical applications, based on the present research to improve SPR biosensors. The main objective of this review is an ultra-sensitive plasmon resonance nano biosensor on a surface based on SMQDs for biomedical applications. This article is divided into three topics: an introduction to SPR and SPR biosensors; explanation and characteristics of SMQDs; and SPR biosensors based on SMQDs. Accordingly, this review clearly presents the characteristics of SMQDs for the development of SPR biosensors and their biomedical applications. In summary, the team believes that this article can highlight current research directions as well as ways to utilize SMQDs for the efficient improvement of SPR biosensors with a high selectivity and sensitivity in biomedical applications.

## 2. SPR

SPR refers to the collective oscillations of electrons on the surface of metal nanostructures that occur in response to an external stimulus such as light or a charge. When the particle size reaches the order of nanometers, the electron can spontaneously accelerate on the surface of the particle and absorb electromagnetic waves of a certain wavelength; a schematic of this phenomenon is shown in Figure 1a [43–45]. The solutions of nanoparticles of rare metals such as silver and gold (which have a high conductivity) often show a strong absorption band in the visible spectrum. When the solution of these nanoparticles with the same size range is exposed to electromagnetic radiation, part of the radiation is scattered, and part of it is accelerated by the free electrons of the nanoparticles; therefore, in this phenomenon, certain frequencies are absorbed, resulting in an enhancement of the electron resonance and appearing as a strong peak in the visible region. The shape and frequency of the resonance spectrum depend on the size, shape, and distance between the nanoparticles and their dielectric properties but, most importantly, on the dielectric properties of the environment in which the nanoparticles are located [46–48]. Figure 1b shows the steps of a typical SPR method. Each sensor-level measurement begins with the selection of a suitable buffer solution, which is the most basic task before starting the association process. At this stage, the sensor surface contains active ligands ready to accept the target analytes. By injecting the solution containing the analytes, the association cycle begins. If the correct ligands are not selected, special bonds can form between the ligands and the analytes after the solution has passed, leading to the instability and detachment of the ligands from the surface. In this step, the kinetic energy resulting from the interaction of analytes and ligands is measured in real time. In the next step, a solution is brought into contact with the sensor surface to regenerate the initial state. As shown in Figure 1b, this step destroys the non-specific binding elements so that the mass accumulated on the surface can be recovered from the sensor reaction. At this stage, analyte dissociation also begins, and the kinetic energy of the dissociation process can be studied. Finally, the regeneration solution is injected, breaking the link between ligands and analytes. If the ligands are properly placed on the surface, they will remain on the surface after passing the regeneration solution as the analytes are gradually removed [49,50].

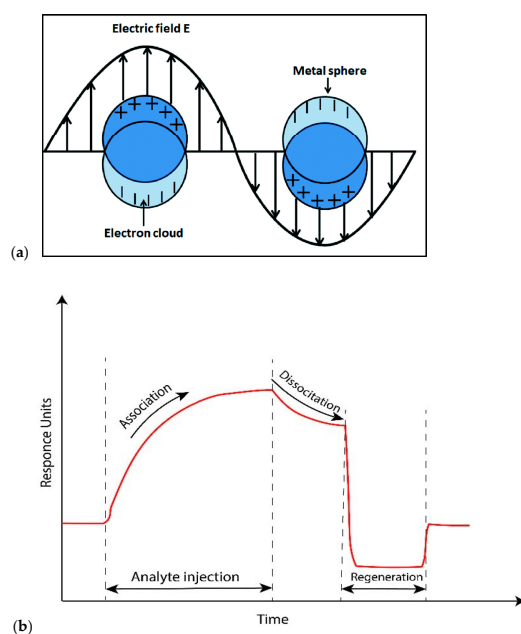


**Figure 1.** (a) Schematic of the surface plasmon (electronic cloud) resonated due to the electric field. (Reprinted with permission [51]. Copyright © 2016, The Author(s). Licensee: IntechOpen.) (b) Steps in a typical SPR method. (Reprinted with permission [49] Copyright © 2020 by the authors. Licensee MDPI, Basel, Switzerland).

### *Biosensor Using SPR*

The light beam propagates in a medium with a larger refractive index  $n_1$  and reaches the common section of a material that has a lower index with a refractive form than the first medium, i.e.,  $n_2$  ( $n_1 > n_2$ ). At an incidence angle greater than the limit angle ( $\theta$ ), the light is completely reflected and returns to the environment with a higher refractive index [52–55]. Additionally, no energy is lost during the reflection of the beam, and the light beam causes the penetration of an electric field intensity into the material with a low refractive index, which is introduced as an evanescent wave. The ‘P-polarized’ component of the evanescent subject can penetrate the metal layer and excite electromagnetic surface plasmon waves that are propagated inside the conductive surface associated with a material with a low refractive index if the total internal reflection interface is covered with a layer of appropriate conductive materials, such as metal with an acceptable thickness. This ‘surface plasmon wave’ has P polarization for a non-magnetic metal, namely, ‘gold’, and because of its electromagnetic properties and diffusion surface, it generates an amplified evanescent wave in comparison to incident electromagnetic waves. If the size and directions of the ‘photon wave’ vector  $k_x$  and the plasmon wave vector  $k_{sp}$  are equal for waves of the same frequency, an amplified evanescent field is produced. When this condition occurs at the landing angle  $\theta$ , the ‘intensity of reflection’ at the angle  $\theta$  can be zero due to the conversion of the energy into a ‘surface’ electric field. With increasing penetration into the thinner material  $n_2$ , the loss in this evanescent field wave’s amplitude is approximately half the wavelength of its resonance away from the surface. To put it another way, the field loss for visible light is of the order of several hundred nanometers. As a result, just the quenching zone is used to investigate analyte molecules. The SPR biosensor is a group of optical biosensors that have advantages such as real-time detection, a short response time, the simultaneous detection of several types of analytes, and non-labeled sensors [56–59]. Exciting surface plasmon waves and their characteristics depend on the electromagnetic properties of the dielectric metal interface. Resonance coupling causes a valley in the reflection spectrum at the SPR resonance angle. SPR biosensing can be obtained by the absorption of ‘target analytes’ on the metal surface and dependent changes in the wavelength and intensity in reflected light. These optical changes can rely on alterations in the refractive index due to the phenomenon of surface absorption. Figure 2 shows the basis of SPR biosensors. The high sensitivity to alterations in the features of the dielectric is caused by the transfer of incident light energy to the ‘surface plasmon wave’ and the resulting high density of the electromagnetic field in the dielectric near the metal layer. The gold metal layer’s penetration depth of 200–300 nanometers offers the chance to detect minute variations in the thickness or ‘refractive index’ of layers on the surface of the metal [60–62]. The resolution limit of SPR biosensors provides the possibility of detecting surfaces with an approximate coverage of 1 picogram/mm [63,64]. Currently, SPR-based biosensors are the most commercialized type of optical biosensors; they usually have large dimensions and high prices and are suitable for laboratory use [65–67]. The technology of surface plasmon resonance sensing as a detector or diagnostic has developed rapidly and has now become an effective tool for direct monitoring and, especially, the analysis of biomolecular interactions. It is also widely used for interactions of biological molecules such as protein–protein supplements, drugs–protein, nucleic acid–protein, nuclear acceptor–DNA, and DNA–DNA. Its fields of application include immunodiagnosis, signal transduction, drug screening, antibody conjugation, and protein conformational changes (Table 1) [56,68].

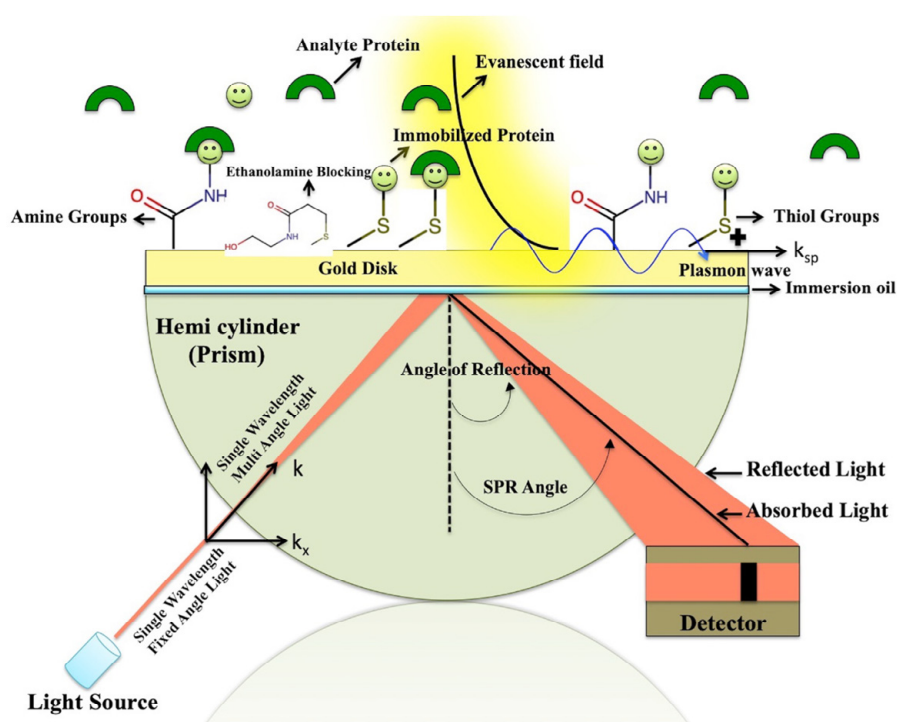


**Figure 2.** The functionality of SPR biosensors. When the analytes interact with the ligands fixed on the ‘surface’, the dielectric index on the gold ‘surface’ changes, and the reflection maximum is seen at a different angle. This angular shift is the result of the interactions between the analyte and the ligand. (Reprinted with permission [69]. Copyright © 2020, Authors. Exclusive licensee: Bio-protoco1 LLC.)

**Table 1.** Applying surface plasmon resonance biosensors in medical diagnosis.

Field	Detection	Species	Ref.
Medical diagnostics	Virus marker	Ebola, Hepatitis B virus	[70,71]
	Cardiac marker	Myoglobin	[72]
	Drug	Warfarin, Morphine	[73,74]
	Cancer marker	Interleukin 8, Prostate-specific antigen	[75,76]

### 3. SMQDs Structure

The aging of the ‘MAX -phase’ ‘A’ layers leads to a layered structure of SMQDs, a new class of 2D materials. These MAX phases consist of a large family of nitrides as well as carbonitrides with the chemical formula  $nAX M_{n+1}$ , where ‘M’ stands for the primary transition metal (such as Sc, Zr, Hf, V, Nb, Mo, Ta, Cr) in layer  $n + 1$ , ‘A’ stands for an element from the periodic table (usually group 13 or even 14), and ‘X’ stands for carbon as well as ‘nitrogen’ in layers X. [77–80]. In Figure 3, all constituent elements of the phase MAX are marked with different colors.



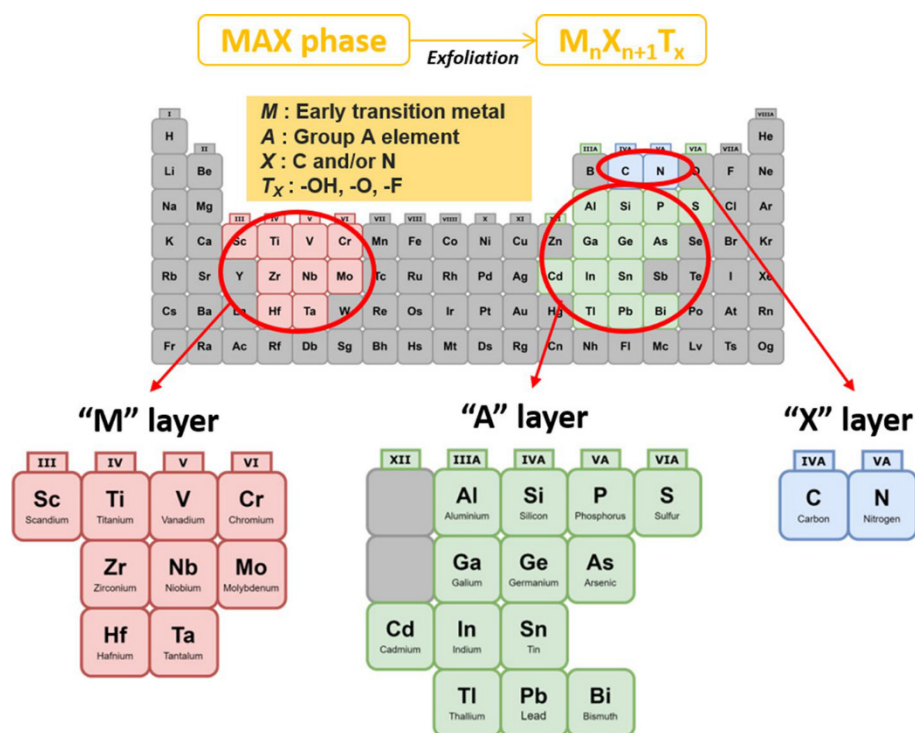


**Figure 3.** Periodic table of the elements that make up the ‘MAX’ phases as well as SMQDs: M: metals with early transition, I: ‘Group A’ element, X: C as well as T<sub>x</sub>, and N: ‘surface function group’. (Reprinted with permission [81]. Copyright © 2021, The Author(s).)

Here, ‘n’ can take the numbers 1, 2, and 3. By changing n from ‘1’ to ‘3’, SMQDs contain layers between three and seven layers of atoms for ‘M<sub>2</sub> ×’, ‘M<sub>3</sub> × 2’, and ‘M<sub>4</sub> × 3’, respectively [82,83]. As shown in Figure 4, during the etching process, the group A element from the MAX phase is replaced by surface groups such as oxygen (–O), hydroxyl (–OH), and fluorine without destroying the MX layers by suitable chemicals [84,85]. In several studies, Ti<sub>3</sub>C<sub>2</sub>T<sub>x</sub> with a surface termination group of -Cl has also been observed, and the general formula is M<sub>n+1</sub>X<sub>n</sub>T<sub>x</sub>, where T is the symbol for the surface groups [86–88]. MAX has ‘layered’ structures in which the bonds between the layers are weaker than the bonds in the layer [89,90]. In other words, the bonds between M and X are a mixture of ionic and covalent bonds, which can be much stronger than the bonds between M and A [91,92]. As a result, the bond between M and A is decomposed at high temperatures, and the 2D structure M<sub>n+1</sub>X<sub>n</sub> is formed. Upon deformation, they become laminated and exhibit a combination of unusual and sometimes unique properties that are intermediate between those of ceramics and metals. For example, like metals, they are capable of conducting electricity and heat, and they can be hard, brittle, and heat-resistant [93,94]. In addition, they are resistant to chemical agents and thermal shocks. However, these ceramics are fabricated as 3D materials, and one of the first experiences with their 2D fabrication is due to ‘2D Ti<sub>3</sub>C<sub>2</sub>’ nanoplatelets. Researchers attempted to remove aluminum from titanium aluminum carbide (Ti<sub>3</sub>AlC<sub>2</sub>) powder by placing it in hydrofluoric acid. Through a chemical process called exfoliation, 2D Ti<sub>3</sub>C<sub>2</sub> nanoplatelets were thus obtained [95,96]. The interesting thing about SMQDs is the naming of this substance. This material is produced from a bulk crystal called Max with the suffix ‘ene’ added to the end, similar to graphene [97,98].

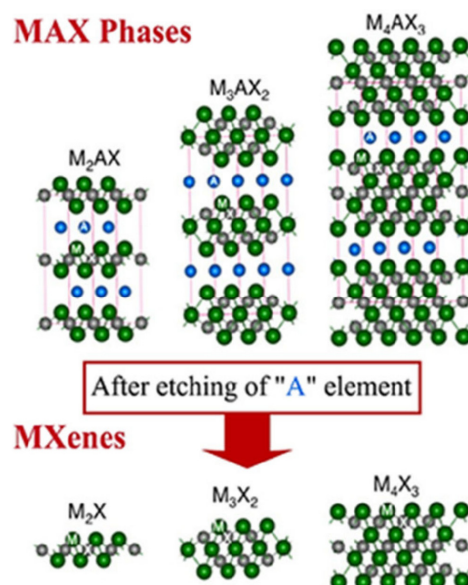


**Figure 4.** Etching of the MAX phase and creation of SMQDs with surface groups. (Reprinted with permission [99] Copyright © 2021 by the authors. Licensee MDPI, Basel, Switzerland.)

### 3.1. Functional Group on the Surface of SMQDs

Surface end groups that are  $-OH$  or  $-O$  replace the A layers by the chemical etching of the MAX phase to produce SMQDs. In these materials, two to four M layers are interspersed with layers of C (carbon) or N (nitrogen) in the clever MXene QD structure. Unlike graphene, the surfaces of these materials have functional groups,  $-O$  or  $-OH$ , that make them hydrophilic. These surface groups are strongly dependent on the etching technique [100,101]. For example,  $Ti_3C_2T_x$  etched with HF has four times more 'F-functional groups' than the material etched with a LiF mixture [102,103]. These functional groups also have a great impact on the detection of the electronic functions of SMQDs. For example, it has been shown that both  $-F$  and  $-OH$  functional groups on the surface of  $Ti_3C_2$  lead to a semiconductor behavior with a band gap of 0.05 to 0.1 eV, while  $Ti_3C_2$  without surface termination exhibits a metallic behavior [104,105]. Moreover, surface functional groups can influence the energy storage application of SMQDs. For example, density functional theory studies confirm that  $Ti_3C_2$  without functional groups stores more lithium ions than its counterpart with a fluorine functional group ( $Ti_3C_2F$ ) because the surface functional groups block lithium adsorption [106,107].

### 3.2. SMQDs Synthesis

The synthesis of SMQDs by precursors is called the top-down method. Depending on the type of precursor, i.e., either MAX or not MAX, this method is divided into two subgroups [100,102]. The most common SMQD precursor is a part of 3D layered carbides as well as nitrides, called the SMQD phase [108,109]. In the precursor materials of the MAX phase, such as  $M_{n+1}AlX_n$  or  $M_{n+1}SiX_n$ , various etching methods are used to break the bonds within the layers and replace the individual elements Al and Si with surface groups [110,111]. Layered materials, where the 'layer-to-layer' bonding is not significantly stronger than the bonding between layers, are divided into one or more atomic layers to produce 2D materials. Ghidui and co-workers [107] argued in 2014 that MAX can be etched with a solution of lithium fluoride and hydrochloric acid or with various amounts of hydrofluoric acid. Table 2 lists various approaches for the synthesis of SMQDs. In general, experimental factors such as the etching time, the particle size of the MAX phase, and the acid concentration used affect the better performance in the preparation of higher-quality SMQDs [33]. Recently, some non-Mex phase precursors have been used to fabricate MXs. For example,  $Zr_3Al_3C_5$  has been used as a precursor, although its constituents are similar to those of Al-bonded MAX phase precursors; however, in this precursor, an 'Al-C' layer

is etched instead of a pure 'Al' layer to produce MXene  $Zr_3C_2$  [112,113]. Considering that both the constituents of the composition and the surface end groups can be changed, the properties and characteristics of SMQDs can also be easily modified [114,115].

**Table 2.** A summary of the different SMQDs synthesis methods.

SMQDs	Functionalization(s)	Synthesis Method of SMQDs	Ref.
Ta <sub>4</sub> C <sub>3</sub>	Manganese oxide (MnOx), 'soy bean' phospholipid (SP)	HF etching	[116]
Ti <sub>3</sub> C <sub>2</sub>	Poly 'lactic-co- glycolic acid' (PLGA), SP, IONPs	HF etching, TPAOH intercalation	[117]
TiO <sub>2</sub> -Ti <sub>3</sub> C <sub>2</sub>	Hemoglobin (Hb), Nafion	Hydrothermal synthesis	[118,119]
Ti <sub>3</sub> C <sub>2</sub>	Cobalt nanowires (CoNWs), Dox	LiF + HCl etching	[120]
Ti <sub>3</sub> C <sub>2</sub> QDs	–	Hydrothermal synthesis	[121]
Ti <sub>2</sub> N QDs	SP	KF + HCl etching, sonication in NMP	[122]
Nb <sub>2</sub> C QDs	–	HF etching, TPAOH sonication (ultrasoundassisted)	[123]

### 3.3. Characteristics and Features of SMQDs

The SMQD material has very interesting properties; for example, although it falls into the category of ceramics, unlike many others, it has good electrical conductivity, which makes it suitable for biomedical applications. The electronic properties of SMQDs are of particular importance because they can be tailored by changing the 'elemental' composition of the SMQDs or the surface functional groups. Other factors such as the band gap can also affect the electronic properties of SMQDs. Unlike graphene, SMQD is hydrophilic, which can be very advantageous in many applications. It is also flexible, pliable, and soft. Because of these properties, it can be formed into complex shapes (its use in the form of a tube or a sheet for materials with a conductivity as high as that of metals is very undesirable) [124,125].

### 3.4. Preparing Hybrid NPs Using SMQDs

A SMQDs composite with tiny magnetic Fe<sub>3</sub>O<sub>4</sub> NPs with a size of about ~4.9 nm (Ti<sub>3</sub>C<sub>2</sub>T<sub>x</sub>/Fe<sub>3</sub>O<sub>4</sub>/TiO<sub>2</sub>) was prepared in an 'aqueous' solution of vitamin C and Fe<sup>3+</sup> salt for 5 h at 150 °C in a stainless steel autoclave with Teflon coating by the hydrothermal method. It is also possible to selectively enrich different biomolecules/antigens based on affinity interactions through these hybrid magnetic NPs. Another interesting alternative for nanocomposites is the combination of SMQDs sheets and metal NPs, which are modified by crosslinkers to detect target molecules due to their strong affinity for SMQDs or other biomolecules [126–128]. SMQDs/metal nanoparticle-based nanocomposites can be prepared using an external reducing agent such as NaBH<sub>4</sub> or the reduction of noble metal salts. To form particles showing surface-enhanced Raman spectroscopy (SERS), the spontaneous reduction of metal salts such as silver, gold, and palladium is applied to Ti<sub>3</sub>C<sub>2</sub>T<sub>x</sub> SMQDs sheets [129] to form NPs. In addition, it is possible to increase the detection sensitivity of oncomarkers such as microRNA using an AuNP/SMQDs composite [130]. The composite has also been used to detect important small bioactive compounds [131] and electrochemical catalysis [132]. The formation of a composite with SMQDs is also possible using graphite oxide as another 2D material, and such a composite for sensor-based applications leads to the maintenance of the biological activity of hemoglobin even after inkjet printing, as well as the stable and efficient electrochemical detection of H<sub>2</sub>O<sub>2</sub> [133].

## 4. SPR Biosensors Based on SMQDs

Along with other 2D materials, SMQDs are a potential biosensor application material. In biosensing, the unique benefits of SMQDs include their biocompatibility and minimal cytotoxicity. In addition, MXenes provide a wide adsorption range for optical detection and enhanced DNA interaction [134,135]. MXenes are also related with metallic conductivity,



intrinsic surface functionalization, and hydrophilic characteristics, all of which may increase the efficacy of SPR biosensors based on MXenes. The features of MXene that make it necessary for biosensors are summarized in Figure 5a.  $\text{Ti}_3\text{C}_2$ , among other compounds, has been extensively documented. Few studies have been conducted on additional MXenes and their composites with metallic nanoparticles, particularly in immunosensing.  $\text{Ti}_3\text{C}_2$ , a member of the MXenes and titanium families, is used in a variety of applications, including SPR biosensors. Numerous publications on the diverse uses of  $\text{Ti}_3\text{C}_2$  MXenes in electrochemical and optical smart biosensors have been published [136–140]. Although MXenes have been widely investigated, the biosensor applications of  $\text{Ti}_2\text{C}$ -MXenes, particularly their composites with nanoparticles, have received less attention (e.g., Au, Ag, etc.). Wang et al. described the production and optical characteristics of  $\text{Ti}_2\text{C}@\text{Au}$  core-shell nanosheets for photonic applications [141]. Zhu et al. built a bifunctional smart nanosensor platform based on Au-Ag nanoshuttles (NSs), utilizing  $\text{Ti}_2\text{C}$  for the electrochemical and SERS measurement of ultratrace carbendazim (CBZ) residues in tea and rice for environmental monitoring [142]. The mechanisms behind SPR biosensors based on SMQDs usually utilize the exclusive ‘electrocatalytic’ properties of the MXene sheet with respect to the relationship of the ‘target signal’ (Figure 5b) [143]. The electronic properties and current signal change when biological targets are attached to SMQDs films. The 2D layered nanostructure provides a large surface area to accommodate biological materials. The electrocatalytic properties change and lead to a linear response when biological components can be immobilized by functional groups on SMQDs nanocomposites. SPR biosensors built on smart MXene QDs have impeccable repeatability, stability, and reproducibility. The use of functional groups enriched on the surface of SMQDs material could be a potential solution, since non-covalent interactions and physical adsorption are not sustainable for some biomedical applications. This would allow for surface bonding in new and controllable ways to alter surface properties [144–148].

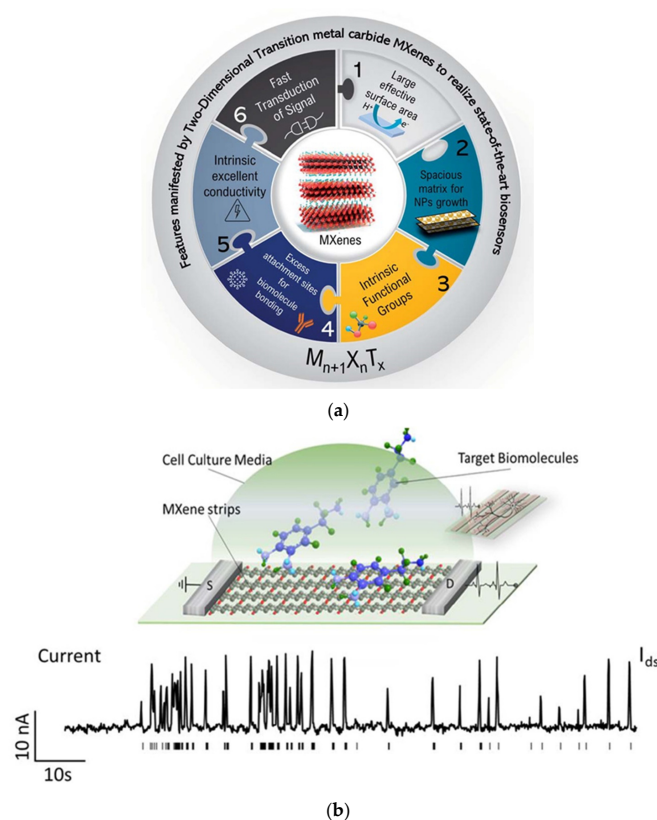


**Figure 5.** (a) Schematic representation of the main features of MXenes with regard to their application in biosensors. (Reprinted with permission [149]. This journal is © The Royal Society of Chemistry 2022.) (b) Mechanisms of the SPR biosensors based on SMQDs groups. (Reprinted with permission [150]. Copyright © 2020, Author(s). Published by IOP Publishing Ltd.)

## 5. Advanced 2D SMQDs-Based SPR Nanobiosensors as Ultra-Sensitive Detection Gadgets

The use of biosensing platforms that use nanomaterials or nanostructures with exceptional optical, magnetic, electrical, mechanical, and electrocatalytic capabilities promotes the link between advancing detection and routine testing. Incorporating new multifunctional nanoscale structures, morphologies, and controlled structures and a large surface-to-volume ratio enables immobilization in bioreceptors while maintaining biostability, biocompatibility, and biodistribution [151]. Therefore, the SPR sensing strategy using nanomaterials can not only be used as an effective tool for the detection of difficult-to-detect molecules in the concentration range between pmol and amol, but it also facilitates the improvement of sensing properties [152]. It is expected that the design of SPR biosensors is promising for the ultrasensitive and selective detection of cancer. 2D layered materials such as SMQDs have anisotropic electron transport behavior and a large surface area, which makes them potential transducer materials for biosensing applications [153–155]. The results of Wu et al. show an increase in the sensitivity of an SPR biosensor by about 25% with ten graphene layers [156]. Gupta et al. also investigated an SPR biosensor with graphene and silicon to increase the sensitivity [157], and their results showed a maximum sensitivity of  $\sim 134.6^\circ/\text{RIU}$ . Ouyang et al. investigated an SPR biosensor with  $\text{MoS}_2$  and silicon to increase the sensitivity [158], and the highest sensitivity was  $\sim 125.44^\circ/\text{RIU}$ . Wu et al. investigated a novel SPR biosensor with  $\text{Ti}_3\text{C}_2\text{Tx-MXene}$  multilayers to increase the sensitivity. According to their results, the sensitivity can reach  $224.5^\circ/\text{RIU}$  [159]. SMQDs nanomaterials exhibit a unique combination of excellent mechanical properties, an ease of functionalization, an excellent electrical conductivity, an extremely thin 2D sheet-like morphology, etc. compared to other 2D materials such as graphite carbon nitride,  $\text{MoS}_2$ , and graphene [160,161]. Among the properties that significantly affect the strength, sensitivity, and selectivity of a biosensor are the inherent properties of the bioreceptor, including its tendency to be structurally stable during the operation of the biosensor, the analyte, and the method used to stabilize the bioreceptor on the surface of the transducer. The bioreceptor component is often attached to a surface, placing it in close proximity to the transducer. Additional requirements that must be met for improved biosensor performance include the interfacial density of the bioreceptor and the distance between the bioreceptor and the transducer (surface). Aptamers, antibodies, enzymes, and protein molecules can be used to influence the design of biosensors based on 2D SMQDs nanomaterials to improve biocompatibility and increase the transporter surface area of the biosensor in conjunction with the increased activity of the catalyst [162–164]. In addition, the implementation of SMQDs as next-generation diagnostic devices requires a significant improvement in the stability of SMQDs against oxidation. Biosensors are small, portable analytical instruments that convert a biochemical process into a quantitative, analytical signal. Because of their high ‘specificity’, small size, and ease of use, biosensors are the preferred instruments for biological components and chemical detection. Biosensors consist of two parts: a bio-detection component that uses a biological element (enzymes, antibodies, nucleic acids, etc.) that interacts with an analyte in a specific biochemical manner, and transducers in which the interaction is converted into quantifiable signals. The integration of the bio-receptor into a suitable matrix for the interaction between analytes and such receptors are the two main obstacles to the improvement of biosensors [165]. Chen et al. designed a new SPR biosensor using thiol-functionalized niobium carbide MXene QDs (referred to as  $\text{Nb}_2\text{C-SH QDs}$ ) as a bio-platform for the N58 aptamer targeting the N gene. As shown in Figure 6, this biosensor was investigated for the sensitive detection of the N gene in various complex environments (e.g., human serum). By the solvothermal method,  $\text{Nb}_2\text{C-QDs}$  were obtained from  $\text{Nb}_2\text{C-MXene}$  nanosheets and then modified with thiol groups (Figure 6a). The  $\text{Nb}_2\text{C-SH QDs}$  were homogeneously distributed on the surface of the chip due to the self-assembly effect between  $\text{Nb}_2\text{C-SH QD}$  and the SPR gold chip, and the N58 aptamer was stabilized by hydrogen bonding,  $\pi$ - $\pi^*$  stacking, and electrostatic adsorption. In the presence of SARS-CoV-2, it is also possible to form a G-quadruplex between the N58 aptamer and the N gene of SARS-CoV-2. Thus, upon binding to the N gene, the structure of the aptamer strands is altered, resulting in

an increase in the contact area or the distance between the probe molecule and the chip. These changes were then translated into changes in the SPR signal for the detection of the SARS-CoV-2 N gene (Figure 6b) [166].

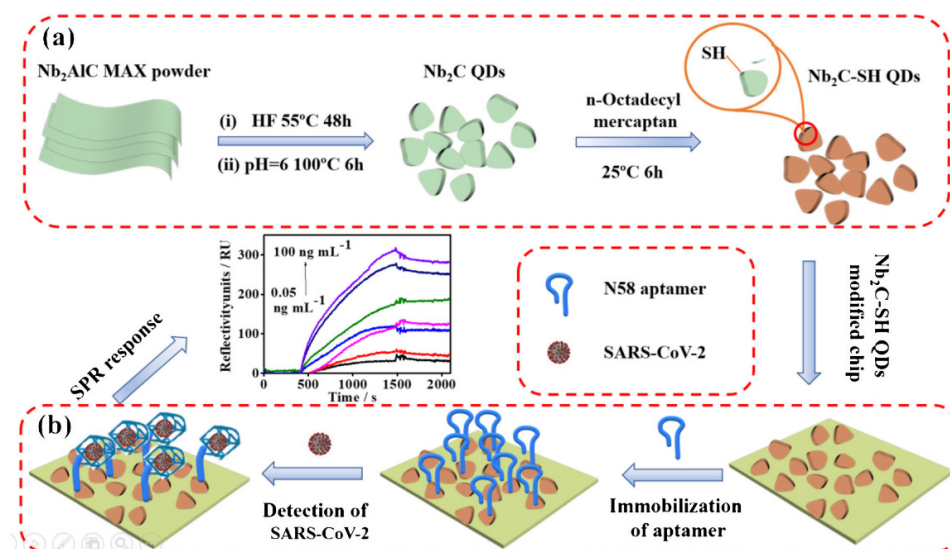


**Figure 6.** (a) Synthesis of Nb<sub>2</sub>C-SH QDs. (b) Fabrication of an Nb<sub>2</sub>C-SH QD-based SPR aptasensor for SARS-CoV-2 N-gene detection. (Reprinted by permission [166]. Copyright © 2022, Springer Nature Switzerland AG. Part of Springer Nature.)

### 5.1. MXene-Based Electro-Chemical SPR Nanobiosensors

Electro-chemical biosensors can be promising selective tools for detecting cancer diseases in the early stages [167]. SWV (square wave voltammetry), CV (cyclic voltammetry), DPV (differential-pulse-voltammetry), and EIS (electro-chemical impedance spectroscopy) are among the electro-chemical methods [168–170]. ‘Lab-on-chip’ biosensors have been miniaturized instruments used in the biomarker research of tumors, leading to potential clinical properties. The small volume of analytes, the direct miniaturization, and the optically absorbing and fluorescent compounds are among the attractive features of biosensors that use surface nano-architectures with this type of detection. Kumar et al. investigated the covalent binding of bioreceptors to f-Ti<sub>3</sub>C<sub>2</sub> SMQDs for the electro-chemical detection of carcinoembryonic antigen (CEA) as a cancer detector. Single-layer SMQDs (Ti<sub>3</sub>C<sub>2</sub>) nano-sheets were used with 3-aminopropyl tri-ethoxy-silane. The enhancement of antibodies anchoring and faster access to analytes are possible by ultra-thin 2D nano-sheets of single/multilayer Ti<sub>3</sub>C<sub>2</sub> SMQDs. According to the findings, the synthesized biofunctional Ti<sub>3</sub>C<sub>2</sub> SMQDs have a linear detection range of 0.0001–2000 n.g.m L<sup>-1</sup>, with a sensitivity to approximately 37.9 Ang<sup>-1</sup> mL cm<sup>-2</sup> per 10 years [160]. A conductive support for the immobilization of aptamer probes is also employed in 2D SMQDs because of their outstanding electrical conductivity and sizable particular surface areas by a variety of possible binding sites. Lorenkova et al. investigated the electrochemical performance of Ti<sub>3</sub>C<sub>2</sub>T<sub>x</sub>-MXenes as sensors [162]. The results obtained showed that the detection limit of 0.7 nM is comparable to the best result obtained so far, which is 0.3 nM [171]. However, there are few reports on SPR sensors integrated with MXene. A recent theoretical study of an MXene-based SPR sensor showed that the coating layers on the gold film can increase the sensitivity of the gold-based SPR sensor. An RI sensitivity of 160 was achieved with four layers of coated gold film at an excitation wavelength of 633 nm, while it was 137 for the devoid setup [159,172].

### 5.2. SMQDs-Based Optical SPR Nanobiosensors

An important technique for the in situ detection of the affinity of various biomolecules that do not require enzymatic labeling is SPR. SPR optical sensing technology is also useful for biomolecule detection. To make the SPR optical biosensor specific for the analytes of interest, they need to be functionalized by bio-recognition molecules (such as proteins, RNA, DNA, cells, etc.). The adhesion of biomolecules to the optical surface is generally achieved by chemical bonds such as (3-aminopropyl) triethox-ysilane and N-succinimidyl-4-maleimidobutyrate [173–175]. In recent years, 2D transition metal dichalcogenides (TMDs), especially MoS<sub>2</sub>, have attracted the attention of researchers in various scientific fields due to their high optical absorption efficiency, high electron conductivity, and tunable band gap [176,177]. The distinctive features of MoS<sub>2</sub> that make it a potential material for the development of biosensor interfaces include the presence of free sulfur atoms, its hydrophobic nature, and its large surface area [178,179]. In addition, MoS<sub>2</sub> layers are also used to inhibit the oxidation of metal layers such as aluminum in SPR biosensors [180]. Additionally, improved operating parameters using nanomaterials have the potential to develop SPR biosensors [181]. The SPR detection platform offers useful advantages such as the ease of miniaturization, ‘label-free’ and ‘real-time’ detections, and rapid detection for bioassays. Ti<sub>3</sub>C<sub>2</sub>T<sub>x</sub> SMQDs multilayers improve the applicability of SPR biosensors due to their absorption [159]. The ‘gold layer’ SMQDs/WS<sub>2</sub> ‘phosphorus’-based platform, using a monolayer of each nanomaterial, was shown to be a new SPR ‘sensing material’ with an increased sensitivity of 15.6% compared to bare ‘metal films’ [182]. SMQDs-based composites such as g-C<sub>3</sub>N<sub>4</sub>/SMQDs AgNPs containing g-C<sub>3</sub>N<sub>4</sub> as a photocatalyst, SMQDs, and AgNPs as electron mediators enhance the photocatalytic activity. In the interface modified with the nanocomposite, the decrease in the band gap energy and the increase in the optical absorption can be observed thanks to the SPR effect of the ‘deposited silver NP’ [183]. The label-free detection of the bovine serum albumin (BSA) protein using an alternative method of fiber optic SPR probe activation with antibodies was evaluated by Kaushik et al. In this new method, gold-coated fibers were first modified with molybdenum disulfide (MoS<sub>2</sub>) nanosheets. The developed technique enables the direct and chemical-free binding of representative antibodies through hydrophobic interactions and also allows for the amplification of SPR signals by the synergistic effects of MoS<sub>2</sub> and the gold metal thin film. The results showed that the sensitivity of the modified MoS<sub>2</sub> sensing probe was improved with a detection limit of 0.29 µg/mL compared to the optical fiber SPR biosensor without MoS<sub>2</sub> coating [184].

According to Wu et al., employing composites constructed of SMQDs, such as g-C<sub>3</sub>N<sub>4</sub>/SMQDs AgNPs, which include g-C<sub>3</sub>N<sub>4</sub> as a photocatalyst, SMQDs, and AgNPs as an electron mediator, increases the photocatalytic activity. The band gap energy is decreased and the optical absorbance is raised at the nanocomposite modified interface as a result of the deposited silver NPs SPR influence. As a signal amplifier, amino-functionalized N-Ti<sub>3</sub>C<sub>2</sub>-MXene-hollow gold NPs (HGNNPs)—staphylococcal protein A—were employed for the detection of CEA with a L.O.D of 0.15 fM (linear range of 0.001 to 1000 p.M) in SPR (Figure 7) [185].

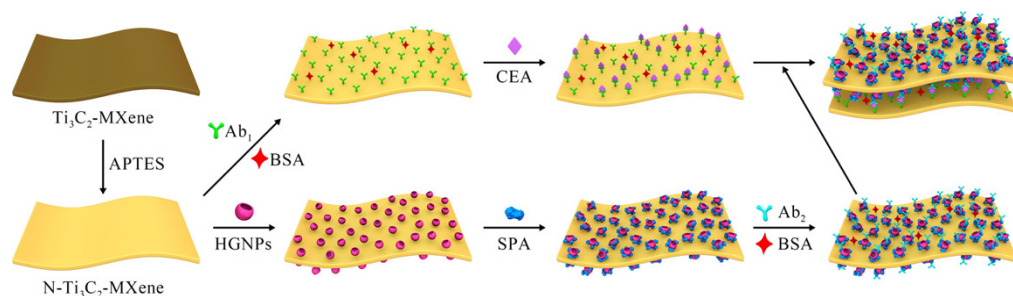


**Figure 7.** Plan of the prepared ‘SPR biosensor’ detection method. (Reprinted with permission [185]. Copyright © 2020, The American Chemical Society.)



## 6. Biomedical Applications of SPR Biosensors Based on SMQDs

SPR biosensors provide a label-free, sensitive, specific, and rapid detection method that is preferred for chemical analysis and medical diagnostics [186]. Over the last three decades, since their beginnings in 1982 as gas sensors [187], SPR biosensors based on 2D nanomaterials such as SMQDs have emerged as suitable sensing platforms for a wide range of applications, e.g., in medicine. Various SPR-based configurations have also been investigated for medical and environmental applications, including SPR biosensors based on SMQDs and fiber-optic SPR sensors [188–190]. Thus, VDW (Weak van der Waals) forces combined with strong ‘hydrogen bonding interactions’ between ‘surface functional groups’ cause SMQDs to assemble into stacked 2D layers [191]. Chemical reactivity and functionalization ability are among the properties of surface functional groups. In biomedical studies, the level of SMQDs is adapted to various materials suitable for cancer treatment and diagnosis, biosensing, antigen detection, drug delivery, and antimicrobial activity (Figure 8) [81]. The medical applications of SMQDs are shown in Table 3.

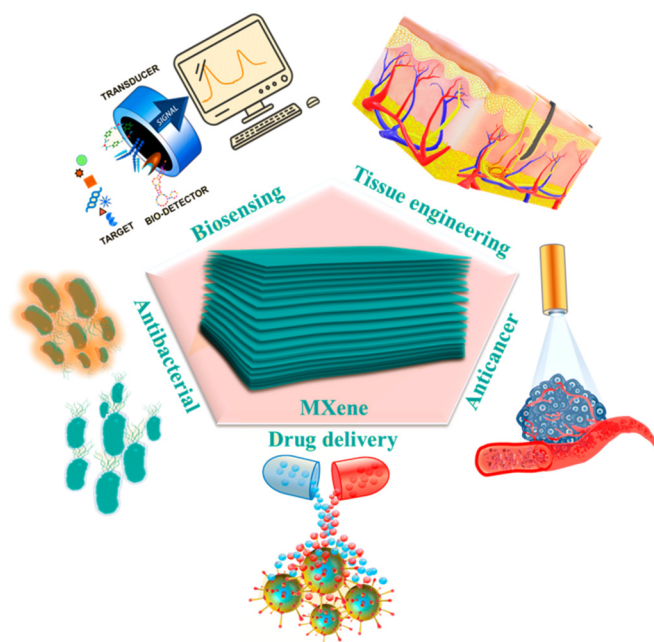


**Figure 8.** Biomedical applications of SMQDs. (Reprinted with permission [192] Copyright © 2022 by the authors. Licensee MDPI, Basel, Switzerland.)

**Table 3.** The medical applications of SMQDs.

SMQDs	Applications	Ref.
Ti <sub>3</sub> C <sub>2</sub>	Detection of curcumin and hypochlorite (ClO <sup>−</sup> )	[193]
Ti <sub>3</sub> C <sub>2</sub>	Glutathione detection and photoelectrochemical biosensing	[194]
V <sub>2</sub> C Quantum dots	(Bio)imaging, photothermal therapy, and tumor detection	[195]
Ti <sub>3</sub> C <sub>2</sub>	Bioimaging, macrophage labeling, and Cu <sup>2+</sup> detection	[196]
2D Nb <sub>2</sub> C-MXenes	Photothermal therapy	[197]
Ti <sub>3</sub> C <sub>2</sub> T <sub>x</sub> -SP	Drug delivery	[198]

### 6.1. Detection of Cancer Biomarkers

SMQDs as new 2D nano-materials have the potential to affect aspects of biosensing such as SPR biosensors in medical applications. Therefore, to detect cancer biomarkers in ‘blood’, SPR biosensors based on SMQDs offer sufficient sensitivity up to ng·m<sup>−1</sup> or



better. In order to simultaneously immobilize biomolecules while resisting non-specific protein binding, much effort should be devoted to finding suitable decoration strategies for SMQDs. These criteria state that, due to their distinct physical and chemical features, SMQDs-based SPR biosensors may be employed to assess complicated substances such as plasma or blood serum (Table 4) [142]. Additionally, the  $Ti_3C_2$  MXene-based SPR biosensor in human serum samples exhibits an ultrasensitive cancer biomarker response with a high recovery, good reproducibility, and good selectivity [161]. Additionally, SMQDs with a high density of functional groups have an ultrathin 2D nano-sheet morphology that can optimize biomolecule loading and speed up access to the analyte. In addition to enabling a larger density of bound biomarkers, which improves biosensor performance, the covalent immobilization of bioreceptors including enzymes, DNA, and proteins can also enhance homogeneity and dispersion [199]. Sundaram et al. studied the engineering of MXenes nitrides and 2D transition metal carbides for the therapy and diagnostics of cancer. The findings show that electro-chemical devices based on MXene have the ability to detect cancer biomarkers and have an extraordinarily high sensitivity in identifying the target analyte [200]. To determine the osteosarcoma cancer biomarker by a microgap dielectrode sensor, the MXene surface on multiple connection triangles was investigated. The detection limit and sensitivity were found to be one fM by having good regression co-efficient values ( $y = 1.0036x + 0.525$ ;  $R^2 = 0.978$ ), and a current increase was found when raising the target DNA concentration. Based on the results of detecting the levels of operating system complications and the quantification of the survivin gene at a lower level, it can be said that the microgap device with the dielectric surface of multiple connection triangles modified with MXene is useful [201].

**Table 4.** SPR nanobiosensor-based SMQDs to detect cancer biomarkers.

MXene-Based Biosensors	Target Biomarker	LOD	Diagnosis Method	Ref.
ssRNA, MoS <sub>2</sub> , AuNPs, Ti <sub>3</sub> C <sub>2</sub> , GCE, and BSA	miRNA-182	0.43 fM	Electrochemical/DPV	[202]
PMo12/PPy@Ti <sub>3</sub> C <sub>2</sub> T <sub>x</sub> /Apt/AE	OPN	0.98 fg m·L <sup>-1</sup>	Electrochemical/EIS	[203]
CD63 aptamer that has been tagged with Cy3 and Ti <sub>3</sub> C <sub>2</sub> MXenes	Exosomes	1.4 × 10 <sup>3</sup> particles m·L <sup>-1</sup>	Ratiometric fluorescence resonance	[204]
M B, DNA, H T, HP 1, AuNPs, Ti <sub>3</sub> C <sub>2</sub> , BiVO <sub>4</sub> , and GCE	VEGF <sub>165</sub>	3.3 fM	Photoelectro-chemical	[205]
MXene/IDE HRP-Au-Ab2-PSA-Ab1	PSA	0.031 ng m·L <sup>-1</sup>	Electrochemical/EIS,CV	[35]
N-Ti <sub>3</sub> C <sub>2</sub> T <sub>x</sub> -MXene	CEA	1.7 pg m·L <sup>-1</sup>	SPR	[206]

### 6.2. Detecting an Exosome as a Supply of Biomarkers of Cancer by Applying 2D SMQDs

Exosome signals transmit in intercellular communications. Additionally, exosomes have the ability to deliver cargo that affects nearby cells and can form pre-metastatic cavities. Exosomes are responsible for the initiation, development, and progression of local malignancies, as well as the formation of metastatic lesions. Exosomes themselves are a popular choice for cancer diagnosis since tumor cells produce more exosomes than normal/healthy cells due to their significantly increased cellular activity [168]. Due to its quick response time, minimal background signal, and high sensitivity, electrochemiluminescence (ECL) has been extensively employed for biomarker research [169]. Because 2D Ti<sub>3</sub>C<sub>2</sub> MXenes nanosheets have a great conductivity, a large surface area, and catalytic characteristics, Zhang et al. studied the possibility of using them as ECL nanoprobe to create a sensitive ECL biosensor to detect exosomes. The results showed that the limit is about 124  $\mu\text{L}^{-1}$  particles, which is more than 100-fold lower than that of the current enzyme-linked immunosorbent assay (ELISA) method (Figure 9) [207].

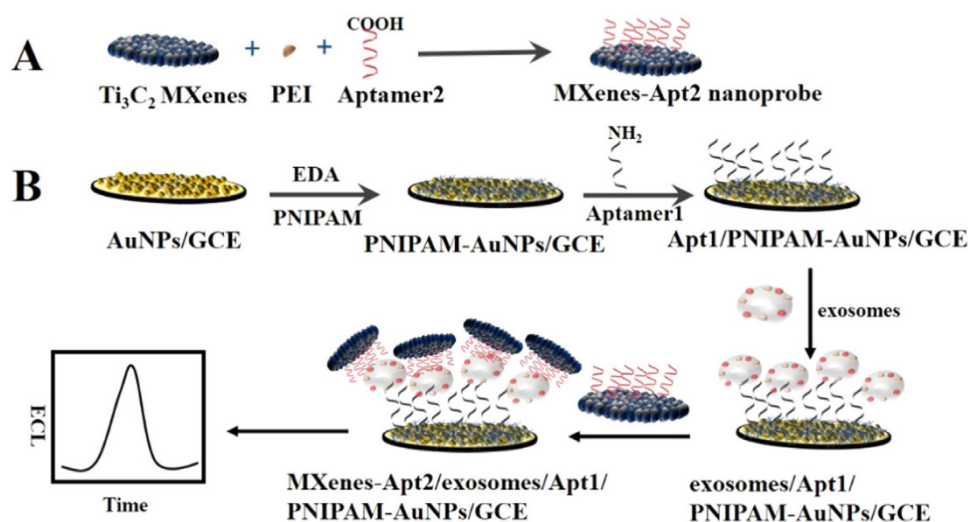


**Figure 9.** ECL biosensor principle for the signal amplification strategy of exosome activity detection. (Reprinted with permission [207]. © 2018 Elsevier B.V. All rights are reserved.)

### 6.3. Detection of Carcinoembryonic Antigen

Carcino-embryonic antigen (CEA) can be one of the cancer markers considered for cancer diagnosis [161].  $\text{Ti}_3\text{C}_2$  SMQDs that are monolayer- or multilayer-coated with an acceptor amino group for covalently immobilizing the carcinoembryonic monoclonal antibody for cancer biomarker detection are the first SMQDs-based CEA detectors. SPR technology, which enables chemical molecules as well as refractive index measurements, has been introduced as a technology to increase the sensitivity of the CEA biosensor [185]. However, due to a lack of quick and accurate diagnostic techniques, it is difficult to identify CEA-related tumors at an early stage, which is essential for effective treatment. SPR biosensor technologies can thus be crucial in reaching this objective [171,172]. While ELISA is traditionally used in scientific settings, SPR biosensors based on SMQDs provide a label-free and real-time detection approach. [208]. SPR biosensors according to SMQDs using genetics [209,210] present in tissue have been used for other ailments that take place at high incidence levels [211]. Liu et al. evaluated the detecting growth differentiation factor-11(GDF11) anti-body using an SPR fiber biosensor based on  $\text{Ti}_3\text{C}_2$  MXenes. They found that the detection of GDF11 after activation with the GDF11 antibody is performed by the fiber SPR sensor, and the sensitivity of the fiber SPR sensor increases to 4804.64 nm/RIU. Likewise, the limit of detection in comparison with the single-molecule ELISA procedure could reach 0.577 pg/L, which is 100-fold lower in comparison with that of the single-molecule ELISA procedure [212]. Altintas et al. studied carcinoembryonic antigen cancer biomarker detection. The results showed that a detection limit of 3 ng/mL CEA was achieved with sustainable detections with a correlation co-efficiency of 1 as well as 0.99 for rabbit anti-mouse (RAM) recording assays [213]. Wu et al. used an SPR biosensor based on 2D transition metal carbide MXene for ultrasensitive CEA detection. They also found that  $\text{Ti}_3\text{C}_2$  MXene, as a novel class of 2D transition metal carbides, provides a large compatible hydrophilic surface that is ideal for SPR biosensing. Based on the results, the dynamic range and detection limit for determining CEA is from  $2 \times 10^{-16}$  to  $2 \times 10^{-8}$  M and 0.07 fM, respectively. Additionally, the results showed that this biosensor approach shows good reproducibility and high specificity for CEA in real serum samples, which provides a promising procedure for evaluating CEA in human serum for the early detection and monitoring of cancer [161].

## 7. Conclusions and Futures Outlooks

In the development of SPR biosensors to achieve high sensitivity and selectivity, numerous nanomaterials have been synthesized and used due to their inherent properties

such as extreme conductivity and plasmonic nature. SMQDs attract a lot of attention in developing SPR biosensors due to their exceptional properties. Accordingly, their potential for biosensor development has been widely investigated since the first reports on SMQDs. Moreover, recent research on the improvement of SPR biosensors based on SMQDs has confirmed that, among various nanomaterials, SMQDs may be the best candidates for the development of various types of biosensors, including fluorescent, optical, and electrochemical biosensors. Moreover, there is still much room for progress in the development of SPR biosensor systems and other next-generation biosensors. These views are supported by recent research on the properties of SMQDs and SPR biosensors based on them. SMQDs improve the performance of SPR biosensors and help in the development of SPR biosensors, as explained in this article. The practical application of these SPR biosensors based on SMQDs faces several challenges, such as the reproducibility of these SPR biosensors and their potential for mass production. However, the commercialization of various SMQDs and the development of SPR biosensors based on SMQDs will depend on ongoing research to develop new synthesis techniques or new SMQD architectures. In addition, it is expected that this ongoing research will lead to a more efficient method of combining SMQDs with other nanomaterials to improve the intrinsic properties of new SMQDs that will be developed in the near future.

**Author Contributions:** S.M.M. and A.G. developed the idea and structure of the review article. V.R., S.A.H. and M.Y.K. wrote the manuscript and collected the materials from databases. C.W.L. and A.G. revised and improved the manuscript. A.G. and W.-H.C. supervised the manuscript. All authors have read and agreed to the published version of the manuscript.

**Funding:** This work is sponsored by the Ministry of Science and Technology, Taiwan (grant number: MOST 110-2628-E-011-003, MOST 109-2923-E-011-003-MY, MOST 111-NU-E-011-001-NU).

**Institutional Review Board Statement:** Not applicable.

**Informed Consent Statement:** Not applicable.

**Data Availability Statement:** All data generated or analyzed during this study are included in this published article.

**Acknowledgments:** This research work was financially supported by the Fundamental Research Grant 529 Scheme FRGS/1/2020/TK0/UM/02/8 (No. FP023-2020) and the Global Collaborative Program—SATU 530 Joint Research Scheme (No. ST004-2021).

**Conflicts of Interest:** The authors declare no conflict of interest.

## References

1. Mehrotra, P. Biosensors and their applications—A review. *J. Oral Biol. Craniofacial Res.* **2016**, *6*, 153–159. [[CrossRef](#)] [[PubMed](#)]
2. Koyun, A.; Ahlatcolu, E.; Koca, Y.; Kara, S. Biosensors and their principles. *A Roadmap Biomed. Eng. Milest.* **2012**, 117–142. [[CrossRef](#)]
3. Pandey, S. *Advance Nanomaterials for Biosensors*; MDPI: Basel, Switzerland, 2022; Volume 12, p. 219.
4. Fan, X.; White, I.M.; Shopova, S.I.; Zhu, H.; Suter, J.D.; Sun, Y. Sensitive optical biosensors for unlabeled targets: A review. *Anal. Chim. Acta* **2008**, *620*, 8–26. [[CrossRef](#)] [[PubMed](#)]
5. Chen, Y.; Ming, H. Review of surface plasmon resonance and localized surface plasmon resonance sensor. *Photonic Sens.* **2012**, *2*, 37–49. [[CrossRef](#)]
6. Cao, J.; Sun, T.; Grattan, K.T. Gold nanorod-based localized surface plasmon resonance biosensors: A review. *Sens. Actuators B Chem.* **2014**, *195*, 332–351. [[CrossRef](#)]
7. Kirsch, J.; Siltanen, C.; Zhou, Q.; Revzin, A.; Simonian, A. Biosensor technology: Recent advances in threat agent detection and medicine. *Chem. Soc. Rev.* **2013**, *42*, 8733–8768. [[CrossRef](#)]
8. Park, Y.M.; Ahn, J.; Choi, Y.S.; Jeong, J.-M.; Lee, S.J.; Lee, J.J.; Choi, B.G.; Lee, K.G. Flexible nanopillar-based immunoelectrochemical biosensor for noninvasive detection of Amyloid beta. *Nano Converg.* **2020**, *7*, 29. [[CrossRef](#)]
9. Alipour, A.; Kalashgarani, M.Y. Nano Protein and Peptides for Drug Delivery and Anticancer Agents. *Adv. Appl. NanoBio-Technol.* **2022**, *3*, 60–64.
10. Roointan, A.; Mir, T.A.; Wani, S.I.; Hussain, K.K.; Ahmed, B.; Abraham, S.; Savardashtaki, A.; Gandomani, G.; Gandomani, M.; Chinnappan, R. Early detection of lung cancer biomarkers through biosensor technology: A review. *J. Pharm. Biomed. Anal.* **2019**, *164*, 93–103. [[CrossRef](#)]

11. Mousavi, S.M.; Hashemi, S.A.; Kalashgrani, M.Y.; Omidifar, N.; Bahrani, S.; Vijayakameswara Rao, N.; Babapoor, A.; Gholami, A.; Chiang, W.-H. Bioactive Graphene Quantum Dots Based Polymer Composite for Biomedical Applications. *Polymers* **2022**, *14*, 617. [[CrossRef](#)]
12. Nunna, B.B.; Mandal, D.; Lee, J.U.; Singh, H.; Zhuang, S.; Misra, D.; Bhuyian, M.N.U.; Lee, E.S. Detection of cancer antigens (CA-125) using gold nano particles on interdigitated electrode-based microfluidic biosensor. *Nano Converg.* **2019**, *6*, 3. [[CrossRef](#)] [[PubMed](#)]
13. Liu, Y.; Yu, D.; Zeng, C.; Miao, Z.; Dai, L. Biocompatible graphene oxide-based glucose biosensors. *Langmuir* **2010**, *26*, 6158–6160. [[CrossRef](#)] [[PubMed](#)]
14. Kazemi, K.; Ghahramani, Y.; Kalashgrani, M.Y. Nano biofilms: An emerging biotechnology applications. *Adv. Appl. NanoBio-Technol.* **2022**, *3*, 8–15.
15. Mousavi, S.M.; Hashemi, S.A.; Gholami, A.; Kalashgrani, M.Y.; Vijayakameswara Rao, N.; Omidifar, N.; Hsiao, W.W.-W.; Lai, C.W.; Chiang, W.-H. Plasma-Enabled Smart Nanoexosome Platform as Emerging Immunopathogenesis for Clinical Viral Infection. *Pharmaceutics* **2022**, *14*, 1054. [[CrossRef](#)]
16. Mohammadniaei, M.; Yoon, J.; Lee, T.; Choi, J.-W. Spectroelectrochemical detection of microRNA-155 based on functional RNA immobilization onto ITO/GNP nanopattern. *J. Biotechnol.* **2018**, *274*, 40–46. [[CrossRef](#)]
17. Elahi, N.; Kamali, M.; Baghersad, M.H.; Amini, B. A fluorescence Nano-biosensors immobilization on Iron (MNPs) and gold (AuNPs) nanoparticles for detection of *Shigella* spp. *Mater. Sci. Eng. C* **2019**, *105*, 110113. [[CrossRef](#)]
18. Mousavi, S.M.; Hashemi, S.A.; Kalashgrani, M.Y.; Gholami, A.; Omidifar, N.; Babapoor, A.; Vijayakameswara Rao, N.; Chiang, W.-H. Recent Advances in Plasma-Engineered Polymers for Biomarker-Based Viral Detection and Highly Multiplexed Analysis. *Biosensors* **2022**, *12*, 286. [[CrossRef](#)]
19. Kalashgrani, M.Y.; Javanmardi, N. Multifunctional Gold nanoparticle: As novel agents for cancer treatment. *Adv. Appl. NanoBio-Technol.* **2022**, *3*, 43–48.
20. Hussein, M.A.; El-Said, W.A.; Abu-Zied, B.M.; Choi, J.-W. Nanosheet composed of gold nanoparticle/graphene/epoxy resin based on ultrasonic fabrication for flexible dopamine biosensor using surface-enhanced Raman spectroscopy. *Nano Converg.* **2020**, *7*, 15. [[CrossRef](#)]
21. Wee, Y.; Park, S.; Kwon, Y.H.; Ju, Y.; Yeon, K.-M.; Kim, J. Tyrosinase-immobilized CNT based biosensor for highly-sensitive detection of phenolic compounds. *Biosens. Bioelectron.* **2019**, *132*, 279–285. [[CrossRef](#)]
22. Mousavi, S.M.; Hashemi, S.A.; Rahmanian, V.; Kalashgrani, M.Y.; Gholami, A.; Omidifar, N.; Chiang, W.-H. Highly Sensitive Flexible SERS-Based Sensing Platform for Detection of COVID-19. *Biosensors* **2022**, *12*, 466. [[CrossRef](#)] [[PubMed](#)]
23. Kalashgrani, M.Y.; Nejad, F.F.; Rahmanian, V. Carbon Quantum Dots Platforms: As nano therapeutic for Biomedical Applications. *Adv. Appl. NanoBio-Technol.* **2022**, *3*, 38–42.
24. Wang, X.; Liu, A.; Xing, Y.; Duan, H.; Xu, W.; Zhou, Q.; Wu, H.; Chen, C.; Chen, B. Three-dimensional graphene biointerface with extremely high sensitivity to single cancer cell monitoring. *Biosens. Bioelectron.* **2018**, *105*, 22–28. [[CrossRef](#)] [[PubMed](#)]
25. Mousavi, S.M.; Hashemi, S.A.; Yari Kalashgrani, M.; Kurniawan, D.; Gholami, A.; Rahmanian, V.; Omidifar, N.; Chiang, W.-H. Recent Advances in Inflammatory Diagnosis with Graphene Quantum Dots Enhanced SERS Detection. *Biosensors* **2022**, *12*, 461. [[CrossRef](#)] [[PubMed](#)]
26. Kalashgrani, M.Y.; Harzand, F.V.; Javanmardi, N.; Nejad, F.F.; Rahmanian, V. Recent Advances in Multifunctional magnetic nano platform for Biomedical Applications: A mini review. *Adv. Appl. NanoBio-Technol.* **2022**, *3*, 31–37.
27. Zhang, H.; Cheng, H.-M.; Ye, P. 2D nanomaterials: Beyond graphene and transition metal dichalcogenides. *Chem. Soc. Rev.* **2018**, *47*, 6009–6012. [[CrossRef](#)]
28. Abootalebi, S.N.; Mousavi, S.M.; Hashemi, S.A.; Shorafa, E.; Omidifar, N.; Gholami, A. Antibacterial effects of green-synthesized silver nanoparticles using *Ferula asafoetida* against *Acinetobacter baumannii* isolated from the hospital environment and assessment of their cytotoxicity on the human cell lines. *J. Nanomater.* **2021**, *2021*, 6676555. [[CrossRef](#)]
29. Sreenilayam, S.P.; Ahad, I.U.; Nicolosi, V.; Brabazon, D. Mxene materials based printed flexible devices for healthcare, biomedical and energy storage applications. *Mater. Today* **2021**, *43*, 99–131. [[CrossRef](#)]
30. Hantanasirisakul, K.; Zhao, M.Q.; Urbankowski, P.; Halim, J.; Anasori, B.; Kota, S.; Ren, C.E.; Barsoum, M.W.; Gogotsi, Y. Fabrication of Ti3C2Tx MXene transparent thin films with tunable optoelectronic properties. *Adv. Electron. Mater.* **2016**, *2*, 1600050. [[CrossRef](#)]
31. Jiang, X.; Kuklin, A.V.; Baev, A.; Ge, Y.; Ågren, H.; Zhang, H.; Prasad, P.N. Two-dimensional MXenes: From morphological to optical, electric, and magnetic properties and applications. *Phys. Rep.* **2020**, *848*, 1–58. [[CrossRef](#)]
32. Kalambate, P.K.; Gadhari, N.S.; Li, X.; Rao, Z.; Navale, S.T.; Shen, Y.; Patil, V.R.; Huang, Y. Recent advances in MXene-based electrochemical sensors and biosensors. *TrAC Trends Anal. Chem.* **2019**, *120*, 115643. [[CrossRef](#)]
33. Sinha, A.; Zhao, H.; Huang, Y.; Lu, X.; Chen, J.; Jain, R. MXene: An emerging material for sensing and biosensing. *TrAC Trends Anal. Chem.* **2018**, *105*, 424–435. [[CrossRef](#)]
34. Tech, J.E.T. Investigating the activity of antioxidants activities content in Apiaceae and to study antimicrobial and insecticidal activity of antioxidant by using SPME Fiber assembly carboxen/polydimethylsiloxane (CAR/PDMS). *J. Environ. Treat. Tech.* **2020**, *8*, 214–224.
35. Chen, J.; Tong, P.; Huang, L.; Yu, Z.; Tang, D. Ti3C2 MXene nanosheet-based capacitance immunoassay with tyramine-enzyme repeats to detect prostate-specific antigen on interdigitated micro-comb electrode. *Electrochim. Acta* **2019**, *319*, 375–381. [[CrossRef](#)]



36. Chen, X.; Sun, X.; Xu, W.; Pan, G.; Zhou, D.; Zhu, J.; Wang, H.; Bai, X.; Dong, B.; Song, H. Ratiometric photoluminescence sensing based on Ti<sub>3</sub>C<sub>2</sub>MXene quantum dots as an intracellular pH sensor. *Nanoscale* **2018**, *10*, 1111–1118. [[CrossRef](#)]
37. Sarycheva, A.; Makaryan, T.; Maleski, K.; Satheeshkumar, E.; Melikyan, A.; Minassian, H.; Yoshimura, M.; Gogotsi, Y. Two-dimensional titanium carbide (MXene) as surface-enhanced Raman scattering substrate. *J. Phys. Chem. C* **2017**, *121*, 19983–19988. [[CrossRef](#)]
38. Mousavi, S.M.; Hashemi, S.A.; Parvin, N.; Gholami, A.; Ramakrishna, S.; Omidifar, N.; Moghadami, M.; Chiang, W.-H.; Mazraedoost, S. Recent biotechnological approaches for treatment of novel COVID-19: From bench to clinical trial. *Drug Metab. Rev.* **2021**, *53*, 141–170. [[CrossRef](#)]
39. Lin, H.; Chen, Y.; Shi, J. Insights into 2D MXenes for versatile biomedical applications: Current advances and challenges ahead. *Adv. Sci.* **2018**, *5*, 1800518. [[CrossRef](#)]
40. Huang, K.; Li, Z.; Lin, J.; Han, G.; Huang, P. Two-dimensional transition metal carbides and nitrides (MXenes) for biomedical applications. *Chem. Soc. Rev.* **2018**, *47*, 5109–5124. [[CrossRef](#)]
41. Dai, C.; Lin, H.; Xu, G.; Liu, Z.; Wu, R.; Chen, Y. Biocompatible 2D titanium carbide (MXenes) composite nanosheets for pH-responsive MRI-guided tumor hyperthermia. *Chem. Mater.* **2017**, *29*, 8637–8652. [[CrossRef](#)]
42. Ahmadi, S.; Fazilati, M.; Nazem, H.; Mousavi, S.M. Green synthesis of magnetic nanoparticles using *Satureja hortensis* essential oil toward superior antibacterial/fungal and anticancer performance. *BioMed Res. Int.* **2021**, *2021*, 8822645. [[CrossRef](#)] [[PubMed](#)]
43. Geldhauser, T.; Ikegaya, S.; Kolloch, A.; Murazawa, N.; Ueno, K.; Boneberg, J.; Leiderer, P.; Scheer, E.; Misawa, H. Visualization of near-field enhancements of gold triangles by nonlinear photopolymerization. *Plasmonics* **2011**, *6*, 207–212. [[CrossRef](#)]
44. Galarreta, B.C.; Harté, E.; Marquestaut, N.; Norton, P.R.; Lagugné-Labarthe, F. Plasmonic properties of Fischer’s patterns: Polarization effects. *Phys. Chem. Chem. Phys.* **2010**, *12*, 6810–6816. [[CrossRef](#)] [[PubMed](#)]
45. Hashemi, S.A.; Mousavi, S.M.; Naderi, H.R.; Bahrani, S.; Arjmand, M.; Hagfeldt, A.; Chiang, W.-H.; Ramakrishna, S. Reinforced polypyrrole with 2D graphene flakes decorated with interconnected nickel-tungsten metal oxide complex toward superiorly stable supercapacitor. *Chem. Eng. J.* **2021**, *418*, 129396. [[CrossRef](#)]
46. Krutyakov, Y.A.; Kudrinsky, A.; Olenin, A.Y.; Lisichkin, G. Synthesis of highly stable silver colloids stabilized with water soluble sulfonated polyaniline. *Appl. Surf. Sci.* **2010**, *256*, 7037–7042. [[CrossRef](#)]
47. Hashemi, S.A.; Mousavi, S.M.; Faghihi, R.; Arjmand, M.; Rahsepar, M.; Bahrani, S.; Ramakrishna, S.; Lai, C.W. Superior X-ray radiation shielding effectiveness of biocompatible polyaniline reinforced with hybrid graphene oxide-iron tungsten nitride flakes. *Polymers* **2020**, *12*, 1407. [[CrossRef](#)]
48. Kelly, K.L.; Coronado, E.; Zhao, L.L.; Schatz, G.C. The Optical Properties of Metal Nanoparticles: The Influence of Size, Shape, and Dielectric Environment. *J. Phys. Chem. B* **2003**, *107*, 668–677. [[CrossRef](#)]
49. Kamal Eddin, F.B.; Fen, Y.W. The principle of nanomaterials based surface plasmon resonance biosensors and its potential for dopamine detection. *Molecules* **2020**, *25*, 2769. [[CrossRef](#)]
50. Schasfoort, R.B. *Handbook of Surface Plasmon Resonance*; Royal Society of Chemistry: London, UK, 2017.
51. Sun, L.; Chen, P.; Lin, L. Enhanced Molecular Spectroscopy via Localized Surface Plasmon Resonance. In *Applications of Molecular Spectroscopy to Current Research in the Chemical and Biological Sciences*; IntechOpen: London, UK, 2016.
52. Homola, J.; Yee, S.S.; Gauglitz, G. Surface plasmon resonance sensors. *Sens. Actuators B Chem.* **1999**, *54*, 3–15. [[CrossRef](#)]
53. Daghestani, H.N.; Day, B.W. Theory and applications of surface plasmon resonance, resonant mirror, resonant waveguide grating, and dual polarization interferometry biosensors. *Sensors* **2010**, *10*, 9630–9646. [[CrossRef](#)]
54. Homola, J. Electromagnetic theory of surface plasmons. In *Surface Plasmon Resonance Based Sensors*; Springer: Berlin/Heidelberg, Germany, 2006; pp. 3–44.
55. Mousavi, S.M.; Low, F.W.; Hashemi, S.A.; Lai, C.W.; Ghasemi, Y.; Soroshnia, S.; Savardashtaki, A.; Babapoor, A.; Pynadathu Rumjit, N.; Goh, S.M. Development of graphene based nanocomposites towards medical and biological applications. *Artif. Cells Nanomed. Biotechnol.* **2020**, *48*, 1189–1205. [[CrossRef](#)] [[PubMed](#)]
56. Yao, Y.; Yi, B.; Xiao, J.; Li, Z. Surface plasmon resonance biosensors and its application. In Proceedings of the 2007 1st International Conference on Bioinformatics and Biomedical Engineering, Wuhan, China, 6–8 July 2007; pp. 1043–1046.
57. Zeng, Y.; Hu, R.; Wang, L.; Gu, D.; He, J.; Wu, S.-Y.; Ho, H.-P.; Li, X.; Qu, J.; Gao, B.Z. Recent advances in surface plasmon resonance imaging: Detection speed, sensitivity, and portability. *Nanophotonics* **2017**, *6*, 1017–1030. [[CrossRef](#)]
58. Martín-Becerra, D.; Armelles, G.; González, M.; García-Martín, A. Plasmonic and magnetoplasmonic interferometry for sensing. *New J. Phys.* **2013**, *15*, 085021. [[CrossRef](#)]
59. Ahmadi, S.; Fazilati, M.; Mousavi, S.M.; Nazem, H. Anti-bacterial/fungal and anti-cancer performance of green synthesized Ag nanoparticles using summer savory extract. *J. Exp. Nanosci.* **2020**, *15*, 363–380. [[CrossRef](#)]
60. Skorobogatiy, M.; Kabashin, A.V. Photon crystal waveguide-based surface plasmon resonance biosensor. *Appl. Phys. Lett.* **2006**, *89*, 143518. [[CrossRef](#)]
61. Arasu, P.; Al-Qazwini, Y.; Onn, B.I.; Noor, A. Fiber Bragg grating based surface plasmon resonance sensor utilizing FDTD for alcohol detection applications. In Proceedings of the 2012 IEEE 3rd International Conference on Photonics, Pulau Pinang, Malaysia, 1–3 October 2012; pp. 93–97.
62. Mousavi, S.; Esmaeili, H.; Arjmand, O.; Karimi, S.; Hashemi, S. Biodegradation study of nanocomposites of phenol novolac epoxy/unsaturated polyester resin/egg shell nanoparticles using natural polymers. *J. Mater.* **2015**, *2015*, 131957. [[CrossRef](#)]



63. Hoa, X.D.; Kirk, A.; Tabrizian, M. Towards integrated and sensitive surface plasmon resonance biosensors: A review of recent progress. *Biosens. Bioelectron.* **2007**, *23*, 151–160. [[CrossRef](#)]
64. Mousavi, S.; Arjmand, O.; Hashemi, S.; Banaei, N. Modification of the epoxy resin mechanical and thermal properties with silicon acrylate and montmorillonite nanoparticles. *Polym. Renew. Resour.* **2016**, *7*, 101–113. [[CrossRef](#)]
65. Samudrala, P.K. Alumina Waveguide Characterization and SPARROW Biosensor Modeling. Graduate Theses, Dissertations, and Problem Reports, 1786. Master's Thesis, West Virginia University, Morgantown, WV, USA, 2006.
66. Nguyen, H.H.; Park, J.; Kang, S.; Kim, M. Surface plasmon resonance: A versatile technique for biosensor applications. *Sensors* **2015**, *15*, 10481–10510. [[CrossRef](#)]
67. Mousavi, S.; Aghili, A.; Hashemi, S.; Goudarzian, N.; Bakhoda, Z.; Baseri, S. Improved morphology and properties of nanocomposites, linear low density polyethylene, ethylene-co-vinyl acetate and nano clay particles by electron beam. *Polym. Renew. Resour.* **2016**, *7*, 135–153. [[CrossRef](#)]
68. Mousavi, S.M.; Hashemi, S.A.; Zarei, M.; Gholami, A.; Lai, C.W.; Chiang, W.H.; Omidifar, N.; Bahrani, S.; Mazraedoost, S. Recent progress in chemical composition, production, and pharmaceutical effects of kombucha beverage: A complementary and alternative medicine. *Evid. -Based Complementary Altern. Med.* **2020**, *2020*, 4397543. [[CrossRef](#)] [[PubMed](#)]
69. Rath, P.P.; Anand, G.; Agarwal, S. Surface Plasmon Resonance Analysis of the Protein-protein Binding Specificity Using Autolab ESPRIT. *Bio-protocol* **2020**, *10*, e3519. [[CrossRef](#)] [[PubMed](#)]
70. Wang, X.; Li, Y.; Wang, H.; Fu, Q.; Peng, J.; Wang, Y.; Du, J.; Zhou, Y.; Zhan, L. Gold nanorod-based localized surface plasmon resonance biosensor for sensitive detection of hepatitis B virus in buffer, blood serum and plasma. *Biosens. Bioelectron.* **2010**, *26*, 404–410. [[CrossRef](#)] [[PubMed](#)]
71. Sharma, P.K.; Kumar, J.S.; Singh, V.V.; Biswas, U.; Sarkar, S.S.; Alam, S.I.; Dash, P.K.; Boopathi, M.; Ganesan, K.; Jain, R. Surface plasmon resonance sensing of Ebola virus: A biological threat. *Anal. Bioanal. Chem.* **2020**, *412*, 4101–4112. [[CrossRef](#)]
72. Gnedenko, O.V.; Mezentsev, Y.V.; Molnar, A.A.; Lisitsa, A.V.; Ivanov, A.S.; Archakov, A.I. Highly sensitive detection of human cardiac myoglobin using a reverse sandwich immunoassay with a gold nanoparticle-enhanced surface plasmon resonance biosensor. *Anal. Chim. Acta* **2013**, *759*, 105–109. [[CrossRef](#)] [[PubMed](#)]
73. Ke, H.; Du, X.; Wang, L.; Wang, X.; Zhu, J.; Gao, Y.; Peng, B.; Hao, H.; Cai, N. Detection of morphine in urine based on a surface plasmon resonance imaging immunoassay. *Anal. Methods* **2020**, *12*, 3038–3044. [[CrossRef](#)]
74. Fitzpatrick, B.; O'Kennedy, R. The development and application of a surface plasmon resonance-based inhibition immunoassay for the determination of warfarin in plasma ultrafiltrate. *J. Immunol. Methods* **2004**, *291*, 11–25. [[CrossRef](#)]
75. Yang, C.-Y.; Brooks, E.; Li, Y.; Denny, P.; Ho, C.-M.; Qi, F.; Shi, W.; Wolinsky, L.; Wu, B.; Wong, D.T. Detection of picomolar levels of interleukin-8 in human saliva by SPR. *Lab A Chip* **2005**, *5*, 1017–1023. [[CrossRef](#)]
76. Ertürk, G.; Özen, H.; Tümer, M.A.; Mattiasson, B.; Denizli, A. Microcontact imprinting based surface plasmon resonance (SPR) biosensor for real-time and ultrasensitive detection of prostate specific antigen (PSA) from clinical samples. *Sens. Actuators B Chem.* **2016**, *224*, 823–832. [[CrossRef](#)]
77. Naguib, M.; Kurtoglu, M.; Presser, V.; Lu, J.; Niu, J.; Heon, M.; Hultman, L.; Gogotsi, Y.; Barsoum, M.W. Two-dimensional nanocrystals produced by exfoliation of  $Ti_3AlC_2$ . *Adv. Mater.* **2011**, *23*, 4248–4253. [[CrossRef](#)]
78. Naguib, M.; Gogotsi, Y. Synthesis of two-dimensional materials by selective extraction. *Acc. Chem. Res.* **2015**, *48*, 128–135. [[CrossRef](#)] [[PubMed](#)]
79. Halim, J. *An X-ray Photoelectron Spectroscopy Study of Multilayered Transition Metal Carbides (MXenes)*; Drexel University: Philadelphia, PA, USA, 2016.
80. Amani, A.M.; Hashemi, S.A.; Mousavi, S.M.; Abrishamifar, S.M.; Vojood, A. Electric field induced alignment of carbon nanotubes: Methodology and outcomes. In *Carbon Nanotubes-Recent Progress*; IntechOpen: London, UK, 2017.
81. Zamhuri, A.; Lim, G.P.; Ma, N.L.; Tee, K.S.; Soon, C.F. MXene in the lens of biomedical engineering: Synthesis, applications and future outlook. *Biomed. Eng. Online* **2021**, *20*, 33. [[CrossRef](#)] [[PubMed](#)]
82. Anasori, B.; Lukatskaya, M.R.; Gogotsi, Y. 2D metal carbides and nitrides (MXenes) for energy storage. *Nat. Rev. Mater.* **2017**, *2*, 16098. [[CrossRef](#)]
83. Hashemi, S.A.; Mousavi, S.M.; Arjmand, M.; Yan, N.; Sundararaj, U. Electrified single-walled carbon nanotube/epoxy nanocomposite via vacuum shock technique: Effect of alignment on electrical conductivity and electromagnetic interference shielding. *Polym. Compos.* **2018**, *39*, E1139–E1148. [[CrossRef](#)]
84. Xu, S.; Liu, W.; Liu, X.; Kuang, X.; Wang, X. A MXene based all-solid-state microsupercapacitor with 3D interdigital electrode. In Proceedings of the 2017 19th International Conference on Solid-State Sensors, Actuators and Microsystems (TRANSDUCERS), Kaohsiung, Taiwan, 18–22 June 2017; pp. 706–709.
85. Mousavi, S.M.; Hashemi, S.A.; Arjmand, M.; Amani, A.M.; Sharif, F.; Jahandideh, S. Octadecyl amine functionalized Graphene oxide towards hydrophobic chemical resistant epoxy Nanocomposites. *ChemistrySelect* **2018**, *3*, 7200–7207. [[CrossRef](#)]
86. Yang, S.; Zhang, P.; Wang, F.; Ricciardulli, A.G.; Lohe, M.R.; Blom, P.W.; Feng, X. Fluoride-free synthesis of two-dimensional titanium carbide (MXene) using a binary aqueous system. *Angew. Chem.* **2018**, *130*, 15717–15721. [[CrossRef](#)]
87. Sun, W.; Shah, S.; Chen, Y.; Tan, Z.; Gao, H.; Habib, T.; Radovic, M.; Green, M. Electrochemical etching of  $Ti_2AlC$  to  $Ti_2CT_x$  (MXene) in low-concentration hydrochloric acid solution. *J. Mater. Chem. A* **2017**, *5*, 21663–21668. [[CrossRef](#)]

88. Mousavi, S.M.; Hashemi, S.A.; Ramakrishna, S.; Esmaeili, H.; Bahrani, S.; Koosha, M.; Babapoor, A. Green synthesis of supermagnetic Fe<sub>3</sub>O<sub>4</sub>-MgO nanoparticles via Nutmeg essential oil toward superior anti-bacterial and anti-fungal performance. *J. Drug Deliv. Sci. Technol.* **2019**, *54*, 101352. [[CrossRef](#)]
89. Nicolosi, V.; Chhowalla, M.; Kanatzidis, M.G.; Strano, M.S.; Coleman, J.N. Liquid exfoliation of layered materials. *Science* **2013**, *340*, 1226419. [[CrossRef](#)]
90. Mousavi, S.M.; Zarei, M.; Hashemi, S.A.; Ramakrishna, S.; Chiang, W.-H.; Lai, C.W.; Gholami, A.; Omidifar, N.; Shokripour, M. Asymmetric membranes: A potential scaffold for wound healing applications. *Symmetry* **2020**, *12*, 1100. [[CrossRef](#)]
91. Abdelmalak, M.N. *MXenes: A New Family of Two-Dimensional Materials and Its Application as Electrodes for Li-ion Batteries*; Drexel University: Philadelphia, PA, USA, 2014.
92. Hashemi, S.A.; Mousavi, S.M. Effect of bubble based degradation on the physical properties of Single Wall Carbon Nanotube/Epoxy Resin composite and new approach in bubbles reduction. *Compos. Part A Appl. Sci. Manuf.* **2016**, *90*, 457–469. [[CrossRef](#)]
93. Naguib, M.; Mashtalir, O.; Carle, J.; Presser, V.; Lu, J.; Hultman, L.; Gogotsi, Y.; Barsoum, M.W. Two-dimensional transition metal carbides. *ACS Nano* **2012**, *6*, 1322–1331. [[CrossRef](#)] [[PubMed](#)]
94. Mousavi, S.M.; Hashemi, S.A.; Jahandideh, S.; Baseri, S.; Zarei, M.; Azadi, S. Modification of phenol novolac epoxy resin and unsaturated polyester using sasobit and silica nanoparticles. *Polym. Renew. Resour.* **2017**, *8*, 117–132. [[CrossRef](#)]
95. Verger, L.; Xu, C.; Natu, V.; Cheng, H.-M.; Ren, W.; Barsoum, M.W. Overview of the synthesis of MXenes and other ultrathin 2D transition metal carbides and nitrides. *Curr. Opin. Solid State Mater. Sci.* **2019**, *23*, 149–163. [[CrossRef](#)]
96. Mousavi, S.M.; Hashemi, S.A.; Amani, A.M.; Saed, H.; Jahandideh, S.; Mojoudi, F. Polyethylene terephthalate/acryl butadiene styrene copolymer incorporated with oak shell, potassium sorbate and egg shell nanoparticles for food packaging applications: Control of bacteria growth, physical and mechanical properties. *Polym. Renew. Resour.* **2017**, *8*, 177–196. [[CrossRef](#)]
97. Barsoum, M.W. *MAX Phases: Properties of Machinable Ternary Carbides and Nitrides*; John Wiley & Sons: Hoboken, NJ, USA, 2013.
98. Mousavi, S.M.; Hashemi, S.A.; Salahi, S.; Hosseini, M.; Amani, A.M.; Babapoor, A. *Development of Clay Nanoparticles toward Bio and Medical Applications*; IntechOpen: London, UK, 2018.
99. Shi, Z.; Khaledialidusti, R.; Malaki, M.; Zhang, H. MXene-based materials for solar cell applications. *Nanomaterials* **2021**, *11*, 3170. [[CrossRef](#)]
100. Verger, L.; Natu, V.; Carey, M.; Barsoum, M.W. MXenes: An introduction of their synthesis, select properties, and applications. *Trends Chem.* **2019**, *1*, 656–669. [[CrossRef](#)]
101. Mousavi, S.M.; Hashemi, S.A.; Esmaeili, H.; Amani, A.M.; Mojoudi, F. Synthesis of Fe<sub>3</sub>O<sub>4</sub> nanoparticles modified by oak shell for treatment of wastewater containing Ni (II). *Acta Chim. Slov.* **2018**, *65*, 750–756. [[CrossRef](#)]
102. Hope, M.A.; Forse, A.C.; Griffith, K.J.; Lukatskaya, M.R.; Ghidui, M.; Gogotsi, Y.; Grey, C.P. NMR reveals the surface functionalisation of Ti<sub>3</sub>C<sub>2</sub> MXene. *Phys. Chem. Chem. Phys.* **2016**, *18*, 5099–5102. [[CrossRef](#)]
103. Mousavi, M.; Hashemi, A.; Arjmand, O.; Amani, A.M.; Babapoor, A.; Fateh, M.A.; Fateh, H.; Mojoudi, F.; Esmaeili, H.; Jahandideh, S. Erythrosine adsorption from aqueous solution via decorated graphene oxide with magnetic iron oxide nano particles: Kinetic and equilibrium studies. *Acta Chim. Slov.* **2018**, *65*, 882–894. [[CrossRef](#)]
104. Ahmed, B.; Anjum, D.H.; Gogotsi, Y.; Alshareef, H.N. Atomic layer deposition of SnO<sub>2</sub> on MXene for Li-ion battery anodes. *Nano Energy* **2017**, *34*, 249–256. [[CrossRef](#)]
105. Mousavi, S.; Zarei, M.; Hashemi, S. Polydopamine for biomedical application and drug delivery system. *Med. Chem.* **2018**, *8*, 218–229. [[CrossRef](#)]
106. Berdiyrov, G. Effect of surface functionalization on the electronic transport properties of Ti<sub>3</sub>C<sub>2</sub> MXene. *EPL (Europhys. Lett.)* **2015**, *111*, 67002. [[CrossRef](#)]
107. Mousavi, S.M.; Hashemi, S.A.; Zarei, M.; Bahrani, S.; Savardashtaki, A.; Esmaeili, H.; Lai, C.W.; Mazraedoost, S.; Abassi, M.; Ramavandi, B. Data on cytotoxic and antibacterial activity of synthesized Fe<sub>3</sub>O<sub>4</sub> nanoparticles using Malva sylvestris. *Data Brief* **2020**, *28*, 104929. [[CrossRef](#)] [[PubMed](#)]
108. Sokol, M.; Natu, V.; Kota, S.; Barsoum, M.W. On the chemical diversity of the MAX phases. *Trends Chem.* **2019**, *1*, 210–223. [[CrossRef](#)]
109. Azhdari, R.; Mousavi, S.M.; Hashemi, S.A.; Bahrani, S.; Ramakrishna, S. Decorated graphene with aluminum fumarate metal organic framework as a superior non-toxic agent for efficient removal of Congo Red dye from wastewater. *J. Environ. Chem. Eng.* **2019**, *7*, 103437. [[CrossRef](#)]
110. Barsoum, M.W.; El-Raghy, T.; Farber, L.; Amer, M.; Christini, R.; Adams, A. The topotactic transformation of Ti<sub>3</sub>SiC<sub>2</sub> into a partially ordered cubic Ti (C<sub>0.67</sub>Si<sub>0.06</sub>) phase by the diffusion of Si into molten cryolite. *J. Electrochem. Soc.* **1999**, *146*, 3919. [[CrossRef](#)]
111. Hashemi, S.A.; Mousavi, S.M.; Ramakrishna, S. Effective removal of mercury, arsenic and lead from aqueous media using Polyaniline-Fe<sub>3</sub>O<sub>4</sub>-silver diethyldithiocarbamate nanostructures. *J. Clean. Prod.* **2019**, *239*, 118023. [[CrossRef](#)]
112. Zhou, J.; Zha, X.; Chen, F.Y.; Ye, Q.; Eklund, P.; Du, S.; Huang, Q. A two-dimensional zirconium carbide by selective etching of Al<sub>3</sub>C<sub>3</sub> from nanolaminated Zr<sub>3</sub>Al<sub>3</sub>C<sub>5</sub>. *Angew. Chem. Int. Ed.* **2016**, *55*, 5008–5013. [[CrossRef](#)]
113. Ravanshad, R.; Karimi Zadeh, A.; Amani, A.M.; Mousavi, S.M.; Hashemi, S.A.; Savar Dashtaki, A.; Mirzaei, E.; Zare, B. Application of nanoparticles in cancer detection by Raman scattering based techniques. *Nano Rev. Exp.* **2018**, *9*, 1373551. [[CrossRef](#)]

114. Halim, J.; Cook, K.M.; Naguib, M.; Eklund, P.; Gogotsi, Y.; Rosen, J.; Barsoum, M.W. X-ray photoelectron spectroscopy of select multi-layered transition metal carbides (MXenes). *Appl. Surf. Sci.* **2016**, *362*, 406–417. [[CrossRef](#)]
115. Mousavi, S.M.; Low, F.W.; Hashemi, S.A.; Samsudin, N.A.; Shakeri, M.; Yusoff, Y.; Rahsepar, M.; Lai, C.W.; Babapoor, A.; Soroshnia, S. Development of hydrophobic reduced graphene oxide as a new efficient approach for photochemotherapy. *RSC Adv.* **2020**, *10*, 12851–12863. [[CrossRef](#)]
116. Dai, C.; Chen, Y.; Jing, X.; Xiang, L.; Yang, D.; Lin, H.; Liu, Z.; Han, X.; Wu, R. Two-dimensional tantalum carbide (MXenes) composite nanosheets for multiple imaging-guided photothermal tumor ablation. *ACS Nano* **2017**, *11*, 12696–12712. [[CrossRef](#)] [[PubMed](#)]
117. Lin, H.; Wang, X.; Yu, L.; Chen, Y.; Shi, J. Two-dimensional ultrathin MXene ceramic nanosheets for photothermal conversion. *Nano Lett.* **2017**, *17*, 384–391. [[CrossRef](#)] [[PubMed](#)]
118. Wang, F.; Yang, C.; Duan, M.; Tang, Y.; Zhu, J. TiO<sub>2</sub> nanoparticle modified organ-like Ti<sub>3</sub>C<sub>2</sub> MXene nanocomposite encapsulating hemoglobin for a mediator-free biosensor with excellent performances. *Biosens. Bioelectron.* **2015**, *74*, 1022–1028. [[CrossRef](#)] [[PubMed](#)]
119. Liu, H.; Duan, C.; Yang, C.; Shen, W.; Wang, F.; Zhu, Z. A novel nitrite biosensor based on the direct electrochemistry of hemoglobin immobilized on MXene-Ti<sub>3</sub>C<sub>2</sub>. *Sens. Actuators B Chem.* **2015**, *218*, 60–66. [[CrossRef](#)]
120. Liu, Y.; Han, Q.; Yang, W.; Gan, X.; Yang, Y.; Xie, K.; Xie, L.; Deng, Y. Two-dimensional MXene/cobalt nanowire heterojunction for controlled drug delivery and chemo-photothermal therapy. *Mater. Sci. Eng. C* **2020**, *116*, 111212. [[CrossRef](#)]
121. Xue, Q.; Zhang, H.; Zhu, M.; Pei, Z.; Li, H.; Wang, Z.; Huang, Y.; Huang, Y.; Deng, Q.; Zhou, J. Photoluminescent Ti<sub>3</sub>C<sub>2</sub> MXene quantum dots for multicolor cellular imaging. *Adv. Mater.* **2017**, *29*, 1604847. [[CrossRef](#)]
122. Shao, J.; Zhang, J.; Jiang, C.; Lin, J.; Huang, P. Biodegradable titanium nitride MXene quantum dots for cancer phototheranostics in NIR-I/II biowindows. *Chem. Eng. J.* **2020**, *400*, 126009. [[CrossRef](#)]
123. Yang, G.; Zhao, J.; Yi, S.; Wan, X.; Tang, J. Biodegradable and photostable Nb<sub>2</sub>C MXene quantum dots as promising nanofluorophores for metal ions sensing and fluorescence imaging. *Sens. Actuators B Chem.* **2020**, *309*, 127735. [[CrossRef](#)]
124. Novoselov, K.S.; Colombo, L.; Gellert, P.R.; Schwab, M.G.; Kim, K. A roadmap for graphene. *Nature* **2012**, *490*, 192–200. [[CrossRef](#)]
125. Hashemi, S.A.; Mousavi, S.M.; Bahrani, S.; Ramakrishna, S. Integrated polyaniline with graphene oxide-iron tungsten nitride nanoflakes as ultrasensitive electrochemical sensor for precise detection of 4-nitrophenol within aquatic media. *J. Electroanal. Chem.* **2020**, *873*, 114406. [[CrossRef](#)]
126. Rakhi, R.; Nayak, P.; Xia, C.; Alshareef, H.N. Novel amperometric glucose biosensor based on MXene nanocomposite. *Sci. Rep.* **2016**, *6*, 36422. [[CrossRef](#)] [[PubMed](#)]
127. Jiang, Y.; Zhang, X.; Pei, L.; Yue, S.; Ma, L.; Zhou, L.; Huang, Z.; He, Y.; Gao, J. Silver nanoparticles modified two-dimensional transition metal carbides as nanocarriers to fabricate acetylcholinesterase-based electrochemical biosensor. *Chem. Eng. J.* **2018**, *339*, 547–556. [[CrossRef](#)]
128. Song, D.; Jiang, X.; Li, Y.; Lu, X.; Luan, S.; Wang, Y.; Li, Y.; Gao, F. Metal-organic frameworks-derived MnO<sub>2</sub>/Mn<sub>3</sub>O<sub>4</sub> microcuboids with hierarchically ordered nanosheets and Ti<sub>3</sub>C<sub>2</sub> MXene/Au NPs composites for electrochemical pesticide detection. *J. Hazard. Mater.* **2019**, *373*, 367–376. [[CrossRef](#)] [[PubMed](#)]
129. Satheeshkumar, E.; Makaryan, T.; Melikyan, A.; Minassian, H.; Gogotsi, Y.; Yoshimura, M. One-step solution processing of Ag, Au and Pd@MXene hybrids for SERS. *Sci. Rep.* **2016**, *6*, 32049. [[CrossRef](#)] [[PubMed](#)]
130. Mohamadzadeh, M.; Koyappayil, A.; Sun, Y.; Min, J.; Lee, M.-H. Gold nanoparticle/MXene for multiple and sensitive detection of oncomiRs based on synergetic signal amplification. *Biosens. Bioelectron.* **2020**, *159*, 112208. [[CrossRef](#)] [[PubMed](#)]
131. Lorencova, L.; Bertok, T.; Filip, J.; Jerigova, M.; Velic, D.; Kasak, P.; Mahmoud, K.A.; Tkac, J. Highly stable Ti<sub>3</sub>C<sub>2</sub>T<sub>x</sub> (MXene)/Pt nanoparticles-modified glassy carbon electrode for H<sub>2</sub>O<sub>2</sub> and small molecules sensing applications. *Sens. Actuators B Chem.* **2018**, *263*, 360–368. [[CrossRef](#)]
132. Filip, J.; Zavarh, S.; Lorencova, L.; Bertok, T.; Yousaf, A.B.; Mahmoud, K.A.; Tkac, J.; Kasak, P. Tailoring electrocatalytic properties of Pt nanoparticles grown on Ti<sub>3</sub>C<sub>2</sub>T<sub>x</sub> MXene surface. *J. Electrochem. Soc.* **2019**, *166*, H54. [[CrossRef](#)]
133. Zheng, J.; Diao, J.; Jin, Y.; Ding, A.; Wang, B.; Wu, L.; Weng, B.; Chen, J. An inkjet printed Ti<sub>3</sub>C<sub>2</sub>-GO electrode for the electrochemical sensing of hydrogen peroxide. *J. Electrochem. Soc.* **2018**, *165*, B227. [[CrossRef](#)]
134. Li, R.; Zhang, L.; Shi, L.; Wang, P. MXene Ti<sub>3</sub>C<sub>2</sub>: An effective 2D light-to-heat conversion material. *ACS Nano* **2017**, *11*, 3752–3759. [[CrossRef](#)] [[PubMed](#)]
135. Manzanares-Palenzuela, C.L.; Pourrahimi, A.M.; Gonzalez-Julian, J.; Sofer, Z.; Pykal, M.; Otyepka, M.; Pumera, M. Interaction of single- and double-stranded DNA with multilayer MXene by fluorescence spectroscopy and molecular dynamics simulations. *Chem. Sci.* **2019**, *10*, 10010–10017. [[CrossRef](#)] [[PubMed](#)]
136. Ramanavicius, S.; Ramanavicius, A. Progress and insights in the application of MXenes as new 2D nano-materials suitable for biosensors and biofuel cell design. *Int. J. Mol. Sci.* **2020**, *21*, 9224. [[CrossRef](#)]
137. Wu, X.; Ma, P.; Sun, Y.; Du, F.; Song, D.; Xu, G. Application of MXene in electrochemical sensors: A review. *Electroanalysis* **2021**, *33*, 1827–1851. [[CrossRef](#)]
138. Li, X.; Lu, Y.; Liu, Q. Electrochemical and optical biosensors based on multifunctional MXene nanoplateforms: Progress and prospects. *Talanta* **2021**, *235*, 122726. [[CrossRef](#)]
139. Thenmozhi, R.; Maruthasalamoorthy, S.; Nirmala, R.; Navamathavan, R. MXene Based Transducer for Biosensor Applications. *J. Electrochem. Soc.* **2021**, *168*, 117507. [[CrossRef](#)]



140. Shahzad, F.; Zaidi, S.A.; Naqvi, R.A. 2D transition metal carbides (MXene) for electrochemical sensing: A review. *Crit. Rev. Anal. Chem.* **2022**, *52*, 848–864. [[CrossRef](#)]
141. Wang, Y.; Liu, S.; Zhu, F.; Gan, Y.; Wen, Q. MXene Core-Shell Nanosheets: Facile Synthesis, Optical Properties, and Versatile Photonics Applications. *Nanomaterials* **2021**, *11*, 1995. [[CrossRef](#)] [[PubMed](#)]
142. Zhu, X.; Liu, P.; Xue, T.; Ge, Y.; Ai, S.; Sheng, Y.; Wu, R.; Xu, L.; Tang, K.; Wen, Y. A novel graphene-like titanium carbide MXene/Au–Ag nanoshuttles bifunctional nanosensor for electrochemical and SERS intelligent analysis of ultra-trace carbendazim coupled with machine learning. *Ceram. Int.* **2021**, *47*, 173–184. [[CrossRef](#)]
143. Xu, B.; Zhu, M.; Zhang, W.; Zhen, X.; Pei, Z.; Xue, Q.; Zhi, C.; Shi, P. Ultrathin MXene-micropattern-based field-effect transistor for probing neural activity. *Adv. Mater.* **2016**, *28*, 3333–3339. [[CrossRef](#)]
144. Amstad, E.; Textor, M.; Reimhult, E. Stabilization and functionalization of iron oxide nanoparticles for biomedical applications. *Nanoscale* **2011**, *3*, 2819–2843. [[CrossRef](#)] [[PubMed](#)]
145. Chimene, D.; Alge, D.L.; Gaharwar, A.K. Two-dimensional nanomaterials for biomedical applications: Emerging trends and future prospects. *Adv. Mater.* **2015**, *27*, 7261–7284. [[CrossRef](#)]
146. Li, X.; Shan, J.; Zhang, W.; Su, S.; Yuwen, L.; Wang, L. Recent advances in synthesis and biomedical applications of two-dimensional transition metal dichalcogenide nanosheets. *Small* **2017**, *13*, 1602660. [[CrossRef](#)] [[PubMed](#)]
147. Svenson, S.; Tomalia, D.A. Dendrimers in biomedical applications—Reflections on the field. *Adv. Drug Deliv. Rev.* **2012**, *64*, 102–115. [[CrossRef](#)]
148. Thanh, N.T.; Green, L.A. Functionalisation of nanoparticles for biomedical applications. *Nano Today* **2010**, *5*, 213–230. [[CrossRef](#)]
149. Babar, Z.U.D.; Della Ventura, B.; Velotta, R.; Iannotti, V. Advances and emerging challenges in MXenes and their nanocomposites for biosensing applications. *RSC Adv.* **2022**, *12*, 19590–19610. [[CrossRef](#)]
150. Xu, B.; Zhi, C.; Shi, P. Latest advances in MXene biosensors. *J. Phys. Mater.* **2020**, *3*, 031001. [[CrossRef](#)]
151. Zamora-Galvez, A.; Morales-Narváez, E.; Mayorga-Martinez, C.C.; Merkoçi, A. Nanomaterials connected to antibodies and molecularly imprinted polymers as bio/receptors for bio/sensor applications. *Appl. Mater. Today* **2017**, *9*, 387–401. [[CrossRef](#)]
152. Zeng, S.; Baillargeat, D.; Ho, H.-P.; Yong, K.-T. Nanomaterials enhanced surface plasmon resonance for biological and chemical sensing applications. *Chem. Soc. Rev.* **2014**, *43*, 3426–3452. [[CrossRef](#)]
153. Taniselass, S.; Arshad, M.M.; Gopinath, S.C. Graphene-based electrochemical biosensors for monitoring noncommunicable disease biomarkers. *Biosens. Bioelectron.* **2019**, *130*, 276–292. [[CrossRef](#)]
154. Majd, S.M.; Salimi, A.; Ghasemi, F. An ultrasensitive detection of miRNA-155 in breast cancer via direct hybridization assay using two-dimensional molybdenum disulfide field-effect transistor biosensor. *Biosens. Bioelectron.* **2018**, *105*, 6–13. [[CrossRef](#)] [[PubMed](#)]
155. Cai, S.; Xiao, W.; Duan, H.; Liang, X.; Wang, C.; Yang, R.; Li, Y. Single-layer Rh nanosheets with ultrahigh peroxidase-like activity for colorimetric biosensing. *Nano Res.* **2018**, *11*, 6304–6315. [[CrossRef](#)]
156. Wu, L.; Chu, H.-S.; Koh, W.S.; Li, E.-P. Highly sensitive graphene biosensors based on surface plasmon resonance. *Opt. Express* **2010**, *18*, 14395–14400. [[CrossRef](#)] [[PubMed](#)]
157. Verma, R.; Gupta, B.D.; Jha, R. Sensitivity enhancement of a surface plasmon resonance based biomolecules sensor using graphene and silicon layers. *Sens. Actuators B Chem.* **2011**, *160*, 623–631. [[CrossRef](#)]
158. Ouyang, Q.; Zeng, S.; Dinh, X.-Q.; Coquet, P.; Yong, K.-T. Sensitivity enhancement of MoS<sub>2</sub> nanosheet based surface plasmon resonance biosensor. *Procedia Eng.* **2016**, *140*, 134–139. [[CrossRef](#)]
159. Wu, L.; You, Q.; Shan, Y.; Gan, S.; Zhao, Y.; Dai, X.; Xiang, Y. Few-layer Ti<sub>3</sub>C<sub>2</sub>T<sub>x</sub> MXene: A promising surface plasmon resonance biosensing material to enhance the sensitivity. *Sens. Actuators B Chem.* **2018**, *277*, 210–215. [[CrossRef](#)]
160. Kumar, S.; Lei, Y.; Alshareef, N.H.; Quevedo-Lopez, M.; Salama, K.N. Biofunctionalized two-dimensional Ti<sub>3</sub>C<sub>2</sub> MXenes for ultrasensitive detection of cancer biomarker. *Biosens. Bioelectron.* **2018**, *121*, 243–249. [[CrossRef](#)]
161. Wu, Q.; Li, N.; Wang, Y.; Xu, Y.; Wei, S.; Wu, J.; Jia, G.; Fang, X.; Chen, F.; Cui, X. A 2D transition metal carbide MXene-based SPR biosensor for ultrasensitive carcinoembryonic antigen detection. *Biosens. Bioelectron.* **2019**, *144*, 111697. [[CrossRef](#)]
162. Lorencova, L.; Bertok, T.; Dosekova, E.; Holazova, A.; Paprckova, D.; Vikartovska, A.; Sasinkova, V.; Filip, J.; Kasak, P.; Jerigova, M. Electrochemical performance of Ti<sub>3</sub>C<sub>2</sub>T<sub>x</sub> MXene in aqueous media: Towards ultrasensitive H<sub>2</sub>O<sub>2</sub> sensing. *Electrochim. Acta* **2017**, *235*, 471–479. [[CrossRef](#)]
163. Gajdosova, V.; Lorencova, L.; Prochazka, M.; Omastova, M.; Micusik, M.; Prochazkova, S.; Kveton, F.; Jerigova, M.; Velic, D.; Kasak, P. Remarkable differences in the voltammetric response towards hydrogen peroxide, oxygen and Ru(NH<sub>3</sub>)<sup>63+</sup> of electrode interfaces modified with HF or LiF-HCl etched Ti<sub>3</sub>C<sub>2</sub>T<sub>x</sub> MXene. *Microchim. Acta* **2020**, *187*, 52. [[CrossRef](#)]
164. Lorencova, L.; Gajdosova, V.; Hroncekova, S.; Bertok, T.; Blahutova, J.; Vikartovska, A.; Parrakova, L.; Gemeiner, P.; Kasak, P.; Tkac, J. 2D MXenes as perspective immobilization platforms for design of electrochemical nanobiosensors. *Electroanalysis* **2019**, *31*, 1833–1844. [[CrossRef](#)]
165. Grieshaber, D.; MacKenzie, R.; Vörös, J.; Reimhult, E. Electrochemical biosensors-sensor principles and architectures. *Sensors* **2008**, *8*, 1400–1458. [[CrossRef](#)]
166. Chen, R.; Kan, L.; Duan, F.; He, L.; Wang, M.; Cui, J.; Zhang, Z.; Zhang, Z. Surface plasmon resonance aptasensor based on niobium carbide MXene quantum dots for nucleocapsid of SARS-CoV-2 detection. *Microchim. Acta* **2021**, *188*, 316. [[CrossRef](#)] [[PubMed](#)]

167. Bertok, T.; Lorencova, L.; Chocholova, E.; Jane, E.; Vikartovska, A.; Kasak, P.; Tkac, J. Electrochemical impedance spectroscopy based biosensors: Mechanistic principles, analytical examples and challenges towards commercialization for assays of protein cancer biomarkers. *ChemElectroChem* **2019**, *6*, 989–1003. [[CrossRef](#)]
168. Lorencova, L.; Bertok, T.; Bertokova, A.; Gajdosova, V.; Hroncekova, S.; Vikartovska, A.; Kasak, P.; Tkac, J. Exosomes as a source of cancer biomarkers: Advances in electrochemical biosensing of exosomes. *ChemElectroChem* **2020**, *7*, 1956–1973. [[CrossRef](#)]
169. Reddy, K.K.; Bandal, H.; Satyanarayana, M.; Goud, K.Y.; Gobi, K.V.; Jayaramudu, T.; Amalraj, J.; Kim, H. Recent trends in electrochemical sensors for vital biomedical markers using hybrid nanostructured materials. *Adv. Sci.* **2020**, *7*, 1902980. [[CrossRef](#)] [[PubMed](#)]
170. Gajdosova, V.; Lorencova, L.; Kasak, P.; Tkac, J. Electrochemical nanobiosensors for detection of breast cancer biomarkers. *Sensors* **2020**, *20*, 4022. [[CrossRef](#)]
171. Xiao, F.; Zhao, F.; Zhang, Y.; Guo, G.; Zeng, B. Ultrasonic electrodeposition of gold-platinum alloy nanoparticles on ionic liquid–chitosan composite film and their application in fabricating nonenzyme hydrogen peroxide sensors. *J. Phys. Chem. C* **2009**, *113*, 849–855. [[CrossRef](#)]
172. Xu, Y.; Ang, Y.S.; Wu, L.; Ang, L.K. High sensitivity surface plasmon resonance sensor based on two-dimensional MXene and transition metal dichalcogenide: A theoretical study. *Nanomaterials* **2019**, *9*, 165. [[CrossRef](#)]
173. Liu, C.; Cai, Q.; Xu, B.; Zhu, W.; Zhang, L.; Zhao, J.; Chen, X. Graphene oxide functionalized long period grating for ultrasensitive label-free immunosensing. *Biosens. Bioelectron.* **2017**, *94*, 200–206. [[CrossRef](#)]
174. Kaushik, S.; Tiwari, U.; Saini, T.; Pandey, A.; Paul, A.; Sinha, R. Long Period Grating Modified with Fe-Metal Organic Frameworks for Detection of Isopropanol. In Proceedings of the International Conference on Fibre Optics and Photonics, Kanpur, India, 4–8 December 2016.
175. Kaushik, S.; Tiwari, U.; Nilima; Prashar, S.; Das, B.; Sinha, R.K. Label-free detection of *E. coli* bacteria by cascaded chirped long period gratings immunosensor. *Rev. Sci. Instrum.* **2019**, *90*, 025003. [[CrossRef](#)] [[PubMed](#)]
176. Singh, E.; Kim, K.S.; Yeom, G.Y.; Nalwa, H.S. Two-dimensional transition metal dichalcogenide-based counter electrodes for dye-sensitized solar cells. *RSC Adv.* **2017**, *7*, 28234–28290. [[CrossRef](#)]
177. Mishra, A.K.; Mishra, S.K.; Verma, R.K. Graphene and beyond graphene MoS<sub>2</sub>: A new window in surface-plasmon-resonance-based fiber optic sensing. *J. Phys. Chem. C* **2016**, *120*, 2893–2900. [[CrossRef](#)]
178. Tuteja, S.K.; Duffield, T.; Neethirajan, S. Liquid exfoliation of 2D MoS<sub>2</sub> nanosheets and their utilization as a label-free electrochemical immunoassay for subclinical ketosis. *Nanoscale* **2017**, *9*, 10886–10896. [[CrossRef](#)]
179. Lee, J.; Dak, P.; Lee, Y.; Park, H.; Choi, W.; Alam, M.A.; Kim, S. Two-dimensional layered MoS<sub>2</sub> biosensors enable highly sensitive detection of biomolecules. *Sci. Rep.* **2014**, *4*, 7352. [[CrossRef](#)]
180. Xu, Y.; Wu, L.; Ang, L.K. MoS<sub>2</sub>-Based Highly Sensitive Near-Infrared Surface Plasmon Resonance Refractive Index Sensor. *IEEE J. Sel. Top. Quantum Electron.* **2018**, *25*, 2868795.
181. Kumar, R.; Pal, S.; Verma, A.; Prajapati, Y.; Saini, J. Effect of silicon on sensitivity of SPR biosensor using hybrid nanostructure of black phosphorus and MXene. *Superlattices Microstruct.* **2020**, *145*, 106591. [[CrossRef](#)]
182. Srivastava, A.; Verma, A.; Das, R.; Prajapati, Y. A theoretical approach to improve the performance of SPR biosensor using MXene and black phosphorus. *Optik* **2020**, *203*, 163430. [[CrossRef](#)]
183. Ding, X.; Li, C.; Wang, L.; Feng, L.; Han, D.; Wang, W. Fabrication of hierarchical g-C<sub>3</sub>N<sub>4</sub>/MXene-AgNPs nanocomposites with enhanced photocatalytic performances. *Mater. Lett.* **2019**, *247*, 174–177. [[CrossRef](#)]
184. Kaushik, S.; Tiwari, U.K.; Deep, A.; Sinha, R.K. Two-dimensional transition metal dichalcogenides assisted biofunctionalized optical fiber SPR biosensor for efficient and rapid detection of bovine serum albumin. *Sci. Rep.* **2019**, *9*, 6987. [[CrossRef](#)]
185. Wu, Q.; Li, N.; Wang, Y.; Xu, Y.; Wu, J.; Jia, G.; Ji, F.; Fang, X.; Chen, F.; Cui, X. Ultrasensitive and selective determination of carcinoembryonic antigen using multifunctional ultrathin amino-functionalized Ti<sub>3</sub>C<sub>2</sub>-MXene nanosheets. *Anal. Chem.* **2020**, *92*, 3354–3360. [[CrossRef](#)]
186. Shrivastav, A.M.; Mishra, S.K.; Gupta, B.D. Fiber optic SPR sensor for the detection of melamine using molecular imprinting. *Sens. Actuators B Chem.* **2015**, *212*, 404–410. [[CrossRef](#)]
187. Liedberg, B.; Nylander, C.; Lunström, I. Surface plasmon resonance for gas detection and biosensing. *Sens. Actuators* **1983**, *4*, 299–304. [[CrossRef](#)]
188. Abdulhalim, I.; Zourob, M.; Lakhtakia, A. Surface plasmon resonance for biosensing: A mini-review. *Electromagnetics* **2008**, *28*, 214–242. [[CrossRef](#)]
189. Singh, P. SPR biosensors: Historical perspectives and current challenges. *Sens. Actuators B Chem.* **2016**, *229*, 110–130. [[CrossRef](#)]
190. Gupta, B.D.; Verma, R.; Srivastava, S.K. *Fiber Optic Sensors Based on Plasmonics*; World Scientific: Singapore, 2015.
191. Zhang, C.J.; Pinilla, S.; McEvoy, N.; Cullen, C.P.; Anasori, B.; Long, E.; Park, S.-H.; Seral-Ascaso, A.; Shmeliov, A.; Krishnan, D. Oxidation stability of colloidal two-dimensional titanium carbides (MXenes). *Chem. Mater.* **2017**, *29*, 4848–4856. [[CrossRef](#)]
192. Koyappayil, A.; Chavan, S.G.; Roh, Y.-G.; Lee, M.-H. Advances of MXenes; Perspectives on Biomedical Research. *Biosensors* **2022**, *12*, 454. [[CrossRef](#)]
193. Liu, M.; Bai, Y.; He, Y.; Zhou, J.; Ge, Y.; Zhou, J.; Song, G. Facile microwave-assisted synthesis of Ti<sub>3</sub>C<sub>2</sub> MXene quantum dots for ratiometric fluorescence detection of hypochlorite. *Microchim. Acta* **2021**, *188*, 15. [[CrossRef](#)]



194. Chen, X.; Li, J.; Pan, G.; Xu, W.; Zhu, J.; Zhou, D.; Li, D.; Chen, C.; Lu, G.; Song, H.  $\text{Ti}_3\text{C}_2$  MXene quantum dots/ $\text{TiO}_2$  inverse opal heterojunction electrode platform for superior photoelectrochemical biosensing. *Sens. Actuators B Chem.* **2019**, *289*, 131–137. [[CrossRef](#)]
195. Cao, Y.; Wu, T.; Zhang, K.; Meng, X.; Dai, W.; Wang, D.; Dong, H.; Zhang, X. Engineered exosome-mediated near-infrared-II region  $\text{V}_2\text{C}$  quantum dot delivery for nucleus-target low-temperature photothermal therapy. *Acs Nano* **2019**, *13*, 1499–1510. [[CrossRef](#)]
196. Guan, Q.; Ma, J.; Yang, W.; Zhang, R.; Zhang, X.; Dong, X.; Fan, Y.; Cai, L.; Cao, Y.; Zhang, Y. Highly fluorescent  $\text{Ti}_3\text{C}_2$  MXene quantum dots for macrophage labeling and  $\text{Cu}^{2+}$  ion sensing. *Nanoscale* **2019**, *11*, 14123–14133. [[CrossRef](#)]
197. Han, X.; Jing, X.; Yang, D.; Lin, H.; Wang, Z.; Ran, H.; Li, P.; Chen, Y. Therapeutic mesopore construction on 2D  $\text{Nb}_2\text{C}$  MXenes for targeted and enhanced chemo-photothermal cancer therapy in NIR-II biowindow. *Theranostics* **2018**, *8*, 4491. [[CrossRef](#)]
198. Han, X.; Huang, J.; Lin, H.; Wang, Z.; Li, P.; Chen, Y. 2D ultrathin MXene-based drug-delivery nanoplatform for synergistic photothermal ablation and chemotherapy of cancer. *Adv. Healthc. Mater.* **2018**, *7*, 1701394. [[CrossRef](#)]
199. Wang, X.D.; Rabe, K.S.; Ahmed, I.; Niemeyer, C.M. Multifunctional silica nanoparticles for covalent immobilization of highly sensitive proteins. *Adv. Mater.* **2015**, *27*, 7945–7950. [[CrossRef](#)]
200. Sundaram, A.; Ponraj, J.S.; Wang, C.; Peng, W.K.; Manavalan, R.K.; Dhanabalan, S.C.; Zhang, H.; Gaspar, J. Engineering of 2D transition metal carbides and nitrides MXenes for cancer therapeutics and diagnostics. *J. Mater. Chem. B* **2020**, *8*, 4990–5013. [[CrossRef](#)]
201. Zhou, D.; Gopinath, S.C.; Saheed, M.S.M.; Sangu, S.S.; LakshmiPriya, T. MXene surface on multiple junction triangles for determining osteosarcoma cancer biomarker by dielectrode microgap sensor. *Int. J. Nanomed.* **2020**, *15*, 10171. [[CrossRef](#)]
202. Liu, L.; Wei, Y.; Jiao, S.; Zhu, S.; Liu, X. A novel label-free strategy for the ultrasensitive miRNA-182 detection based on  $\text{MoS}_2/\text{Ti}_3\text{C}_2$  nanohybrids. *Biosens. Bioelectron.* **2019**, *137*, 45–51. [[CrossRef](#)]
203. Zhou, S.; Gu, C.; Li, Z.; Yang, L.; He, L.; Wang, M.; Huang, X.; Zhou, N.; Zhang, Z.  $\text{Ti}_3\text{C}_2\text{T}_x$  MXene and polyoxometalate nanohybrid embedded with polypyrrole: Ultra-sensitive platform for the detection of osteopontin. *Appl. Surf. Sci.* **2019**, *498*, 143889. [[CrossRef](#)]
204. Zhang, Q.; Wang, F.; Zhang, H.; Zhang, Y.; Liu, M.; Liu, Y. Universal  $\text{Ti}_3\text{C}_2$  MXenes based self-standard ratiometric fluorescence resonance energy transfer platform for highly sensitive detection of exosomes. *Anal. Chem.* **2018**, *90*, 12737–12744. [[CrossRef](#)]
205. Liu, Y.; Zeng, H.; Chai, Y.; Yuan, R.; Liu, H.  $\text{Ti}_3\text{C}_2/\text{BiVO}_4$  Schottky junction as a signal indicator for ultrasensitive photoelectrochemical detection of VEGF 165. *Chem. Commun.* **2019**, *55*, 13729–13732. [[CrossRef](#)]
206. Wen, W.; Qiong, W.; Sheng-Nan, R.; Zhuo, L.; Fang-Fang, C.  $\text{Ti}_3\text{C}_2$ -MXene-assisted signal amplification for sensitive and selective surface plasmon resonance biosensing of biomarker. *Chin. J. Anal. Chem.* **2022**, *50*, 13–18.
207. Zhang, H.; Wang, Z.; Zhang, Q.; Wang, F.; Liu, Y.  $\text{Ti}_3\text{C}_2$  MXenes nanosheets catalyzed highly efficient electrogenerated chemiluminescence biosensor for the detection of exosomes. *Biosens. Bioelectron.* **2019**, *124*, 184–190. [[CrossRef](#)] [[PubMed](#)]
208. Pichersky, E.; Dudareva, N.; Lee, G.Y.; Lim, C.T.; Hatti-Kaul, R.; Törnvall, U.; Gustafsson, L.; Börjesson, P.; Healy, D.A.; Hayes, C.J. 93 Multifunctional cargo systems for biotechnology. *Biotechnology* **2007**, *25*, 89–138.
209. Tombelli, S.; Minunni, M.; Luzi, E.; Mascini, M. Aptamer-based biosensors for the detection of HIV-1 Tat protein. *Bioelectrochemistry* **2005**, *67*, 135–141. [[CrossRef](#)]
210. Gao, Z.; Zhang, J.; Ting, B.P. A doubly amplified electrochemical immunoassay for carcinoembryonic antigen. *Biosens. Bioelectron.* **2009**, *24*, 1825–1830. [[CrossRef](#)]
211. Quershi, A.; Gurbuz, Y.; Kang, W.P.; Davidson, J.L. A novel interdigitated capacitor based biosensor for detection of cardiovascular risk marker. *Biosens. Bioelectron.* **2009**, *25*, 877–882. [[CrossRef](#)]
212. Liu, C.; Wang, R.; Shao, Y.; Chen, C.; Wu, P.; Wei, Y.; Gao, Y. Detection of GDF11 by using a  $\text{Ti}_3\text{C}_2$ -MXene-based fiber SPR biosensor. *Opt. Express* **2021**, *29*, 36598–36607. [[CrossRef](#)]
213. Altintas, Z.; Uludag, Y.; Gurbuz, Y.; Tothill, I.E. Surface plasmon resonance based immunosensor for the detection of the cancer biomarker carcinoembryonic antigen. *Talanta* **2011**, *86*, 377–383. [[CrossRef](#)]